Title: Maintenance of homeostatic plasticity at the Drosophila neuromuscular junction requires continuous IP_3-directed signaling

Authors and Affiliations:

Thomas D. James [1,2], Danielle J. Zwiefelhofer [1], and C. Andrew Frank [1,3]

[1] – Department of Anatomy and Cell Biology, University of Iowa Carver College of Medicine, Iowa City, IA 52242 USA

[2] – Interdisciplinary Graduate Program in Neuroscience, University of Iowa, Iowa City, IA 52242 USA

[3] – Interdisciplinary Programs in Neuroscience, Genetics, and Molecular Medicine, University of Iowa, Iowa City, IA 52242 USA

Address for Correspondence: C. Andrew Frank. Department of Anatomy and Cell Biology, University of Iowa Carver College of Medicine, 51 Newton Road, 1-661A. Iowa City, IA 52242. USA.

andy-frank@uiowa.edu

ABSTRACT

Synapses and circuits rely on neuroplasticity to adjust output and meet physiological needs. Forms of homeostatic synaptic plasticity (HSP) impart stability at synapses by countering destabilizing perturbations. The *Drosophila melanogaster* larval neuromuscular junction (NMJ) is a model synapse with robust expression of HSP. At the NMJ, a homeostatic system detects impaired postsynaptic sensitivity to neurotransmitter and activates a retrograde signal that restores synaptic function by adjusting neurotransmitter release. This process has been separated into temporally distinct phases, induction and maintenance. One prevailing hypothesis is that a shared mechanism governs both phases. Here we show the two phases are separable. Combining genetics, pharmacology, and electrophysiology, we find that a signaling system consisting of PLCβ, inositol triphosphate (IP_3), IP_3 receptors, and Ryanodine receptors is required only for the maintenance of HSP. We also find that the NMJ is capable of inducing homeostatic signaling – even when its sustained maintenance process is absent.

INTRODUCTION

Synaptic plasticity is a fundamental property of neurons that underlies the activities of neuronal circuits and behaviors. Neurons have a remarkable capacity to adjust outputs in response to external cues. Depending upon context, those adjustments can be stabilizing or destabilizing to overall synapse or circuit function. Hebbian forms of neuroplasticity are generally thought to promote destabilizing changes to synaptic function. Decades of research has resulted in a large amount known about the molecular mechanisms underlying Hebbian paradigms of synaptic plasticity like Long Term Potentiation (LTP, e.g. (Lisman et al., 2012)) – and how Hebbian plasticity might underlie long-lasting processes like memory formation and consolidation (Andersen et al., 2017; Poo et al., 2016). By contrast, less is understood about homeostatic forms of neuroplasticity, which work to stabilize synapse function and keep overall activity levels within an acceptable physiological range (Davis, 2006; Davis and Müller, 2015; Pozo and Goda, 2010; Turrigiano, 2017). For homeostatic plasticity, it is generally thought that coordinated actions of both neurons and their targets work to maintain a set point functional parameter.

Well-studied examples of homeostatic synaptic plasticity (HSP) include synaptic scaling (O'Brien et al., 1998; Turrigiano et al., 1998; Turrigiano and Nelson, 2004), and the maintenance of evoked excitation at neuromuscular junctions (NMJs) (Cull-Candy et al., 1980; Davis and Müller, 2015; Frank, 2014a; Petersen et al., 1997). For both examples, the time course of the implementation homeostatic signaling has been of longstanding interest. Synaptic scaling was initially shown to be a slow, chronically executed process (O'Brien et al., 1998; Turrigiano et al., 1998), but it is also possible for fast scaling mechanisms to be mobilized if multiple synaptic sites are concurrently inhibited (Sutton et al., 2006). For the NMJ, homeostatic signaling can be implemented after a short-term challenge to synapse function (Frank et al., 2006; Wang et al., 2016b), but it is also chronically maintained for extended developmental time in the face of long-term challenges to synapse function (Cull-Candy et al., 1980; Davis et al., 1998; DiAntonio et al., 1999; Petersen et al., 1997; Plomp et al., 1992). It is unclear how signaling systems that drive HSP

65 transition from a state of induction to a state of maintenance. It is also not understood how inter-
66 dependent short-term and long-term HSP implementation mechanisms are. A more complete un-
67 derstanding of these fundamental properties of synaptic homeostasis could have important impli-
68 cations for neurological conditions where synapse stability is episodically lost (Russell et al.,
69 2013).

70 The *Drosophila melanogaster* NMJ is an ideal model synapse for studying the basic ques-
71 tion of how synapses work to counter destabilizing perturbations (Frank, 2014a). At the Drosophila
72 NMJ, reduced sensitivity to single vesicles of glutamate initiates a retrograde, muscle-to-nerve
73 signaling cascade that induces increased neurotransmitter vesicle release, or quantal content
74 (QC). As a result, the NMJ maintains a normal postsynaptic response level (Frank et al., 2006;
75 Petersen et al., 1997). Mechanistically, this increase in QC depends upon the successful execu-
76 tion of discrete presynaptic events, such as increases in neuronal Ca^{2+} influx and an increase in
77 the size of the readily releasable pool (RRP) of synaptic vesicles (Frank et al., 2006; Müller and
78 Davis, 2012; Müller et al., 2012). The field has termed this compensatory signaling process as
79 presynaptic homeostatic potentiation (PHP).

80 As part of our goal to understand how PHP is maintained, we previously identified *Plc21C*
81 (Brusich et al., 2015). *Plc21C* encodes a Drosophila Phospholipase Cβ (PLCβ) homolog known
82 to be neuronally expressed (Shortridge et al., 1991), and recent ribosomal profiling data also
83 indicates muscle expression of *Plc21C* (Chen and Dickman, 2017). In canonical signaling path-
84 ways, once PLCβ is activated by Gαq, it cleaves the membrane lipid phosphatidylinositol 4,5-
85 bisphosphate (PIP_2) into diacylglycerol (DAG) and inositol triphosphate (IP_3). DAG can affect syn-
86 aptic function by activating Protein Kinase C (PKC), while IP_3 binds its receptor (IP_3R) to trigger
87 release of calcium from intracellular stores (Kadamur and Ross, 2012; Philip et al., 2010; Tedford
88 and Zamponi, 2006). It is not understood which aspects of this signaling machinery are mobilized
89 during PHP. Potential downstream consequences of PLCβ activity at the NMJ include phosphor-
90 ylation of neuronal proteins, modulation of ion channel activity, and changes in localization of

91 neurotransmission machinery (Cremona and De Camilli, 2001; Goni and Alonso, 1999; Huang et
92 al., 2006; Peters et al., 2001; Rohrbough and Broadie, 2005; Wu et al., 2002).
93 For this study, we scrutinized PLCβ-directed signaling further. We tested whether PLCβ-
94 directed signaling was required solely for the maintenance of PHP or if it could also be required
95 for induction. In addition to PLCβ, we identified the IP_3 Receptor (Drosophila Itpr, herein IP_3R)
96 and Ryanodine receptor (Drosophila RyR) as being part of the same signaling process to maintain
97 PHP. Yet neither PLCβ, nor IP_3R, nor RyR were required for the rapid induction of PHP. Addition-
98 ally, we found that the rapid induction of PHP is still possible in synapses already sustaining PHP.
99 In other words, NMJs can respond to acute impairments while already compensating for chronic
100 impairments by further potentiating neurotransmitter release. Surprisingly, we also found that
101 NMJs are capable of rapidly inducing PHP – even when the sustained expression of PHP is al-
102 ready blocked by impairments in PLCβ, IP_3R, or RyR signaling. Taken together, our data show
103 that the induction and maintenance of PHP are separable. Even though there is compelling evi-
104 dence that induction and maintenance signaling mechanisms overlap (Goel et al., 2017), it is also
105 true that acute PHP is possible in scenarios where long-term PHP is not.
106

107 **MATERIALS AND METHODS**

108 *Drosophila husbandry*

109 *Drosophila melanogaster* fruit flies were raised on Cornmeal, Molasses and Yeast Medium pre-
110 pared according to the Bloomington Drosophila Stock Center (BDSC, Bloomington, IN) recipe.
111 Drosophila husbandry was performed according to standard practices (Greenspan, 2004). Larvae
112 were raised at 25°C or 29°C (as indicated) in humidity controlled and light-controlled Percival DR-
113 36VL incubators (Geneva Scientific).
114

115 *Drosophila genetic lines*

116 w^{1118} (Hazelrigg et al., 1984) was used as a non-transgenic wild type stock. The deletion *GluRIIA*
117 allele ($GluRIIA^{SP16}$) was generated previously (Petersen et al., 1997). *UAS-IP_3-sponge* lines

118 (*UAS-IP$_3$-sponge.m30* and *UAS-IP$_3$-sponge.m49*) were directly provided by Drs. Masayuki Ko-
119 ganezawa and Daisuke Yamamoto (Usui-Aoki et al., 2005). The *UAS-GluRIII[RNAi]* line utilized
120 to screen homeostatic candidate molecules was described previously (Brusich et al., 2015). GAL4
121 drivers simultaneously utilized for the *"Pre- + Post-Gal4"* conditions were *elaV(C155)-Gal4* (Lin
122 and Goodman, 1994), *Sca-Gal4* (Budnik et al., 1996), and *BG57-Gal4* (Budnik et al., 1996).
123 In addition to the *UAS-IP$_3$-sponge* lines, numerous *UAS-RNAi* or genetic mutant lines were
124 obtained either from the BDSC or the Vienna Drosophila Stock Center (VDRC, Vienna, Austria).
125 Those specific mutations and lines are detailed in Supplementary Table 2. Procedures for how
126 the *UAS-RNAi* lines were generated have been published (Dietzl et al., 2007; Ni et al., 2009).
127
128 *Electrophysiology and Pharmacology*
129 Wandering third instar larvae were collected and filleted for NMJ analysis. Activity in abdominal
130 muscle 6 from segments 2 and 3 was recorded in a modified HL3 saline (70 mM NaCl, 5 mM KCl,
131 5 mM HEPES, 10 mM NaHCO3, 115 mM sucrose, 0.5 mM $CaCl_2$ (unless otherwise noted), 10
132 mM MgCl2, 4.2 mM trehalose, pH 7.2) (see (Stewart et al., 1994) for original parameters). Sharp
133 electrode recordings of miniature excitatory postsynaptic potentials (mEPSPs) and excitatory
134 postsynaptic potentials (EPSPs) were conducted as previously described (Brusich et al., 2015;
135 Spring et al., 2016; Yeates and Frank, 2017). Uncorrected quantal content (QC) was estimated
136 per NMJ as average EPSP/average mEPSP and was also reported as corrected for non-linear
137 summation as done previously (Martin, 1955).
138 Pharmacological agents were bath applied at recording saline at the final concentrations
139 indicated in the text, figures, and tables. The agents included Philanthotoxin-433 (PhTox, Sigma-
140 Aldrich and Santa Cruz Biotechnology), Xestospongin C (Abcam), 2-APB (Tocris, Bio-Techne
141 Corporation), Ryanodine (Tocris), and Dantrolene (Tocris)
142
143 *Immunostaining and Analyses*

144 Immunostaining and image analyses of NMJ 6/7 in segments A2 and A3 were performed as pre-
145 viously described (Spring et al., 2016; Yeates and Frank, 2017). Briefly, filleted larvae were fixed
146 in Bouin's fixative for 4 min, washed, incubated in primary antibodies for 2 hours, washed, and
147 incubated in secondary antibodies for an additional 2 hours. Bouton staining was performed to
148 assess NMJ growth by using the following primary antibodies: mouse anti-Synapsin (anti-Syn;
149 3C11) 1:50 (Developmental Studies Hybridoma Bank, Iowa City, IA) and rabbit anti-Dlg 1:15,000
150 (Budnik et al. 1996). The following fluorophore conjugated secondary antibodies were also used
151 (Jackson ImmunoResearch Laboratories): goat anti–mouse 488 1:1000 (DyLight) and goat anti–
152 rabbit 549 1:2000 (Dy-Light). Alexa-647 goat anti-HRP was utilized to immunostain neuronal
153 membranes. Larval preparations were mounted in Vectashield (Vector Laboratories) and imaged
154 at room temperature using Zen software on a Zeiss 880 Laser Scanning Microscope with an EC
155 Plan-Neofluar 40X Oil DIC Objective (aperture 1.30) or an EC Plan-Apochromat 63X Oil DIC
156 Objective (aperture 1.40; Zeiss). Experimental and control larval preps were imaged using iden-
157 tical acquisition settings, and analyzed using the same procedure and thresholds. Images were
158 prepared for publication in Adobe Photoshop using identical procedures for experimental and
159 control images. Anti-Dlg bouton counts were completed in a blinded fashion to quantify synapse
160 growth. For each anti-Dlg–positive bouton counted in muscle, it was verified that there was a
161 corresponding cluster of anti-Syn staining in neurons.
162
163 **RESULTS**
164
165 **PLCβ loss uncouples the short-term induction of homeostatic plasticity from its long-term**
166 **maintenance**
167 Previously we demonstrated that loss-of-function of *Plc21C*, a *Drosophila melanogaster*
168 PLCβ gene, could dampen or eliminate the long-term maintenance of presynaptic homeostatic
169 potentiation (PHP) (Brusich et al., 2015). We started this study by repeating a subset of those
170 experiments. We utilized a fruit fly line containing both neuron- and muscle-GAL4 drivers as well

171 as a *UAS-GluRIII[RNAi]* transgenic construct to provide a chronic homeostatic challenge that re-
172 duces quantal size (Brusich et al., 2015). *Pre-* + *Post-Gal4* >> *UAS-GluRIII[RNAi]* NMJs have
173 decreased quantal size compared to controls and an offsetting, homeostatic increase in quantal
174 content (QC, Fig. 1A) that keeps excitatory postsynaptic potentials (EPSPs) at control levels (Fig.
175 1B; Supplementary Table S1 for Fig. 1 electrophysiological data). By contrast, concurrent knock-
176 down of *GluRIII* and *Plc21C* gene functions by RNAi (*Pre-* + *Post-Gal4* >> *UAS-GluRIII[RNAi]* +
177 *Plc21C[RNAi]*) leaves this form of homeostatic potentiation only partly intact. There is a small QC
178 increase compared to baseline (Fig. 1A), but this QC increase is blunted, resulting in evoked
179 potentials that are significantly smaller than controls (Fig. 1B; Supplementary Table S1). These
180 data are consistent with the prior results (Brusich et al., 2015).

181 We extended this work to test if *Plc21C* gene knock down blocks or impairs the acute
182 induction of PHP. The *GluRIII* RNAi knock down manipulation in muscle is a days-long, chronic
183 homeostatic challenge to the maintenance of NMJ function (Brusich et al., 2015). For acute in-
184 duction of PHP, we applied 20 μM of the glutamate receptor antagonist Philanthotoxin-433
185 (PhTox) to both wild-type and to *Pre-* + *Post-Gal4* >> *Plc21C[RNAi]* knock down NMJs. Acute
186 PhTox application decreased quantal size for both wild-type and *Plc21C* knockdown NMJs (Fig.
187 1C) (Frank et al., 2006). For both genotypes, evoked potentials remained steady in the presence
188 of PhTox because there was a significant, compensatory increase in quantal content (Figs. 1C,
189 D). These data suggested that partial loss of *Plc21C* gene function is not a sufficient condition to
190 block the rapid induction of PHP.

191 The acute induction of PHP and the long-term maintenance of PHP are genetically sepa-
192 rable by *Plc21C* knock down. This result mirrors data for other homeostatic maintenance signaling
193 molecules, such as Target of Rapamycin (TOR) (Goel et al., 2017; Kauwe et al., 2016; Penney
194 et al., 2012) and C-terminal Src Kinase (Spring et al., 2016). Because these temporal phases of
195 PHP are genetically separable by the loss of specific molecules, we next asked whether the ca-
196 pacity to maintain PHP for long periods of developmental time is required for its rapid induction.

197 Our first step was to test if PHP could be rapidly induced in a synapse already chronically
198 sustaining homeostatic potentiation. The most commonly employed modes of inducing PHP at
199 the Drosophila NMJ are a lifelong, genetic *GluRIIA*^{SP16} null mutation (Petersen et al., 1997) and
200 acute PhTox application (Frank et al., 2006). For both cases, mEPSP amplitudes are decreased
201 and QC is increased helping to maintain evoked potentials at (or near) normal levels. PhTox tar-
202 gets the function of GluRIIA-containing receptors; adding PhTox to a *GluRIIA*^{SP16} null background
203 does not further decrease quantal size (Frank et al., 2006). This presents a difficulty in testing
204 whether additional PHP can be acutely induced in a chronic glutamate receptor loss genetic con-
205 dition already sustaining PHP. We reasoned that applying PhTox to *UAS-GluRIII[RNAi]* knock
206 down synapses could circumvent this limitation. At these synapses, partial loss of the essential
207 subunit-encoding *GluRIII* gene leaves some GluRIIA-containing receptors intact (Brusich et al.,
208 2015). In turn, those GluRIIA-containing receptors could be subject to the secondary PhTox chal-
209 lenge.

210 When we applied PhTox to *UAS-GluRIII[RNAi]* synapses, we observed a further decrease
211 in mEPSP amplitude – significantly below the quantal size amplitude recorded for *UAS-*
212 *GluRIII[RNAi]* alone (Figs. 1E, F). In response, we also observed an offsetting increase in QC
213 (Figs. 1E, F). This result indicated that a rapid induction of PHP was possible at a synapse already
214 undergoing a sustained maintenance of PHP.

215 We next tested whether compromised ability to sustain PHP throughout life would pre-
216 clude acute induction of PHP. PhTox treatment applied to NMJs simultaneously expressing both
217 *UAS-GluRIII[RNAi]* and *Plc21C[RNAi]* constructs induced a significant decrease in mEPSP am-
218 plitude relative to non-PhTox-treated control synapses (Figs. 1E, F). Yet we also observed a sig-
219 nificant increase in QC (i.e. PHP induction) which kept evoked NMJ potentials unchanged from
220 their non-PhTox levels, which were depressed due to the impairment of PHP maintenance (Figs.
221 1E, F). These data suggest that successful acute PHP induction does not require intact PHP
222 maintenance.
223

224 **IP_3 function is required for the maintenance of PHP but not its induction**

225 We sought to identify potential PLCβ signaling effectors that could mediate the long-term
226 maintenance of PHP. We examined possible targets by electrophysiological screening. Based on
227 the canonical signaling functions of PLCβ, we conducted a small screen, targeting molecules such
228 as PKC, CaMKII, Unc-13, as well several potential G-protein-coupled receptors (GPCRs). We
229 also tested molecules implicated in intracellular calcium signaling or synaptic ion channel function.

230 We used a screening paradigm we had previously designed in order to find factors needed
231 for the maintenance of PHP: combining pre- and postsynaptic GAL4 expression with *UAS-*
232 *GluRIII[RNAi]* (Brusich et al., 2015). We targeted most factors for this screen using either *UAS-*
233 *gene* misexpression or *UAS-gene[RNAi]* constructs. We also utilized available loss-of-function
234 mutations. For an additional screening condition for some of those mutations we also constructed
235 double mutant lines with a $GluRIIA^{SP16}$ null deletion allele (Petersen et al., 1997). For any screen
236 test, two conditions were analyzed: a baseline neurotransmission condition (e.g., GAL4 + genetic
237 manipulation alone) and a homeostatically challenged condition (e.g., GAL4 + genetic manipula-
238 tion + *UAS-GluRIII[RNAi]*). Any homeostatically challenged condition that failed to increase QC
239 over its own baseline condition was designated as a potential positive.

240 We examined 28 distinct genetic manipulations (comprising 23 distinct genes), including
241 controls (Fig. 2A; Supplementary Table S2 for raw electrophysiological data from the screen). The
242 relative QC values for the screen are shown (Fig. 2A) and plotted as "% baseline", indicating how
243 much of a QC change the *UAS-GluRIII[RNAi]* challenge yielded. We set the cutoff for a "screen
244 positive" as a QC smaller than one standard deviation below expected the expected QC given
245 the *UAS-GluRIII[RNAi]* homeostatic challenge (Fig. 2A, red dashed line).

246 Of the 28 manipulations, only two failed to significantly increase QC upon homeostatic
247 challenge (Fig. 2A, red). In both cases, the screened target molecule was inositol 1,4,5-triphos-
248 phate (IP_3). IP_3 is a second-messenger signaling molecule. PLCβ cleaves the phospholipid PIP_2
249 into soluble IP_3 and membrane-bound diacylglycerol (DAG). We were able to target cellular IP_3
250 signaling by expressing *UAS-IP_3-sponge*, a transgene that expresses a peptide that binds and

251 sequesters IP_3 (Usui-Aoki et al., 2005). Concomitant pre-and postsynaptic expression of two dif-
252 ferent *UAS-IP$_3$-sponge* transgenes both completely blocked the long-term expression of PHP
253 (Fig. 2B). This resulted in significantly smaller EPSP amplitudes in the *UAS-GluRIII[RNAi]* PHP-
254 challenge genetic background. (Fig. 2C).

255 We utilized the full block of sustained PHP afforded by *UAS-IP$_3$-sponge* expression to
256 further test the relationship between the rapid induction of PHP and its long-term expression. First,
257 we tested if *UAS-IP$_3$-sponge* expression alone could block the rapid induction of PHP. Following
258 PhTox treatment, synapses expressing *UAS-IP$_3$-sponge* in pre- and postsynaptic tissues showed
259 a significant decrease in mEPSP amplitude compared to non-PhTox controls, and yet they still
260 had a robust increase in QC (Fig. 2D-F). This result indicated that *UAS-IP$_3$-sponge* expression
261 left the rapid induction mechanisms of PHP intact.

262 We next tested if the rapid induction of PHP was possible for third instar larval NMJs that
263 had blocked PHP maintenance throughout life. To do this, we applied PhTox to NMJs expressing
264 *UAS-IP$_3$-sponge* in a *UAS-GluRIII[RNAi]* background. Even in this genetic background, we found
265 that the rapid induction of PHP remained intact following PhTox treatment (Figs. 2D-F). Specifi-
266 cally, PhTox treatment resulted in a further decrease in mEPSP amplitude compared to non-
267 PhTox-treated synapses expressing both *UAS-GluRIII[RNAi]* and *UAS-IP$_3$-sponge*, but an offset-
268 ting increase in QC. As expected for this genetic background, the evoked event amplitudes did
269 not recover to full wild-type levels (Figs. 2E, F). However, evoked amplitudes did return to levels
270 returned recorded in non-PhTox treated synapses, indicating successful induction of PHP in a
271 genetic background unable to sustain PHP throughout development (Fig. 2E).

272 Chronic expression of the *UAS-IP$_3$-sponge* transgene blocked the long-term expression
273 of PHP. In principle, this result could be a secondary consequence of aberrant NMJ development.
274 To check this possibility, we employed immunofluorescence microscopy, co-immunostaining third
275 instar larval Drosophila NMJs with anti-Synapsin (Syn, presynaptic vesicles), anti-Discs Large
276 (Dlg, postsynaptic density), and anti-Horseradish Peroxidase (HRP, presynaptic membrane) an-
277 tibodies. This allowed us to examine synaptic growth by counting NMJ boutons. We quantified

278 bouton growth for synapse 6/7, muscle segments A2 and A3. We examined control conditions
279 and conditions with blocked PHP maintenance due to *UAS-IP3-sponge* expression (Figs. 3A-E).
280 We observed no significant differences (versus wild-type control) in bouton number for any con-
281 dition, for either segment A2 or A3 – including the genetic background where we co-expressed
282 *UAS-IP3-sponge* and *UAS-GluRIII[RNAi]* (Fig. 3F). These data indicate that when IP_3 is seques-
283 tered, NMJ undergrowth is not causal for the PHP block.
284

285 **Pharmacology targeting IP_3 receptors uncouples the induction and maintenance of PHP**

286 Having identified *UAS-IP_3-sponge* as a reagent capable of blocking the long-term mainte-
287 nance of PHP, we next tested if the temporal requirements of PHP (induction vs. maintenance)
288 could be also be uncoupled by disrupting Drosophila IP_3 receptor function (Itpr in Drosophila,
289 herein IP_3R). IP_3Rs are generally localized to the endoplasmic reticulum (ER) and canonically
290 function by mediating calcium efflux from internal stores (Berridge, 1984, 1987). ER has long been
291 known to localize throughout the neuronal soma in Drosophila (including synapses) (Summerville
292 et al., 2016), and recent studies have implicated ER resident proteins in the execution of PHP at
293 the Drosophila NMJ (Genç et al., 2017; Kikuma et al., 2017). To target IP_3Rs, we turned to phar-
294 macology, using two reagents known to impair IP_3R function: Xestospongin C and 2-APB (2-
295 Aminoethoxydiphenyl Borate) and applying those drugs to *GluRIIA* loss-of-function mutants.

296 Xestospongin C is a membrane-permeable drug that disrupts intracellular calcium release
297 directly via non-competitive inhibition of IP_3Rs (Gafni et al., 1997; Wilcox et al., 1998). It also acts
298 indirectly by inhibiting SERCA, which could lead to depletion of intracellular calcium stores
299 (Castonguay and Robitaille, 2002). Xestospongin C has been previously shown to inhibit Dro-
300 sophila IP_3Rs (Vazquez-Martinez et al., 2003). By electrophysiology, *GluRIIA^{SP16}* null mutant
301 NMJs showed a marked homeostatic increase in QC due to long-term maintenance of PHP (Fig.
302 4A) (Petersen et al., 1997). *GluRIIA^{SP16}* NMJ preparations acutely treated with 20 μM Xestospon-
303 gin C (10 minutes) displayed the expected decrease in mEPSP amplitude compared to controls
304 (Fig. 4A), but these drug-treated NMJs failed to show an increase in QC (Supplementary Table

305 S3 for Fig. 4 electrophysiology data). Thus, not only did Xestospongin C induce a block of PHP
306 maintenance, but it was capable of extinguishing this long-term maintenance process on a time-
307 scale of minutes. Importantly, 20 μM Xestospongin C did not impair baseline neurotransmission
308 in a wild-type background (Fig. 4B). Additionally, in the *GluRIIA* null background, neither a lower
309 dose (5 μM Xestospongin C) nor vehicle application alone inhibited PHP (Fig. 4A).

310 2-APB is a membrane-permeable drug that has variable pharmacological effects. It is
311 known to impair IP_3R (Diver et al., 2001; Maruyama et al., 1997). However, there are also reports
312 that 2-APB can impair targets such as Transient Receptor Potential (TRP) channels (Bootman et
313 al., 2002; Xu et al., 2005). We employed 2-APB as a second pharmacological agent to target
314 IP_3Rs. If continuous IP_3R function were required for the maintenance PHP at NMJs, we reasoned
315 that acute application of 2-APB (as with Xestospongin C) should also extinguish this form of neu-
316 roplasticity. We found that application of either 1 μM or 10 μM 2-APB to *GluRIIA*^{SP16} null NMJs
317 resulted in a failure to increase QC compared to drug-treated wild-type controls (Fig. 4C; vehicle
318 control same as in Fig. 4A), resulting in small evoked events for the drug-treated *GluRIIA*^{SP16}
319 NMJs (Fig. 4D).

320 We note that 2-APB potentiated baseline neurotransmission, seemingly in a dose-depend-
321 ent way (Fig. 4D; Supplementary Table S3). This potentiation likely means that 2-APB had off-
322 target effects at the NMJ in addition to IP_3Rs. However, taken together, our pharmacological data
323 show that with acute drug application, it is possible to erase a lifelong, *GluRIIA*^{SP16}-induced long-
324 term maintenance of PHP. The fact that this can be done with known IP_3R inhibitors suggests that
325 the maintenance of PHP requires continuous IP_3R function.

326 Finally, we tested if the same acute drug application conditions could block the PhTox-
327 induced rapid induction of PHP. We applied 20 μM PhTox to wild-type NMJs, concurrently with
328 either 20 μM Xestospongin C or 1 μM 2-APB. We found that neither Xestospongin C nor 2-APB
329 treatment disrupted the rapid induction of PHP following PhTox application to wild-type synapses
330 (Fig. 4E). As a result, evoked potentials remained at normal levels (Fig. 4F). Collectively, our

331 experiments demonstrate that acute pharmacological perturbations targeting IP_3Rs uncouple the
332 short-term induction and the long-term maintenance of PHP.
333
334 **Pharmacology targeting Ryanodine Receptors uncouples the induction and maintenance**
335 **of PHP**
336 In conjunction with IP_3 receptors, Ryanodine receptors (RyRs) also mediate release of
337 calcium from ER stores (Berridge, 1998; Simkus and Stricker, 2002), and RyRs are localized to
338 the ER in excitable tissues like neurons and muscle (Santulli and Marks, 2015; Santulli et al.,
339 2017). Therefore, we tested whether RyRs are also required for the maintenance of PHP at the
340 NMJ.
341 We repeated the same types of experiments executed with the IP_3R pharmacological
342 blockade – this time targeting Drosophila RyRs by utilizing Ryanodine (Murmu et al., 2010) or
343 Dantrolene (Vazquez-Martinez et al., 2003; Zhao et al., 2001) at concentrations previously re-
344 ported to block RyRs. We acquired similar results as with IP_3R blockade. We found that acute
345 application of either 100 μM Ryanodine or 10 μM Dantrolene to *GluRIIA* null NMJ preparations
346 resulted in failure of PHP maintenance. QC did not increase for the homeostatically challenged
347 condition (*GluRIIA* + drug) versus the unchallenged condition (wild-type + drug) (Fig. 5A; Supple-
348 mentary Table S4 for Fig. 5 electrophysiology data).
349 We next tested whether RyR inhibition could block the rapid induction of PHP. As was the
350 case with IP_3R inhibition, acute application of 10 μM Dantrolene to PhTox-treated NMJs did not
351 disrupt the short-term induction of PHP (Figs. 5B, C). Moreover, we extended our analysis by re-
352 examining the condition where we combined a long-term homeostatic challenge (*GluRIII[RNAi]*)
353 with a short-term challenge (PhTox) to further decrease quantal size (as in Figs. 1E, F). In this
354 double-challenge condition, addition of 10 μM Dantrolene still left the rapid induction portion of
355 PHP intact (Figs. 5B, C). Collectively, these experiments demonstrate that acute pharmacological
356 perturbations targeting RyRs are capable of uncoupling the short-term induction and the long-
357 term maintenance of PHP.

358 In some tissues, RyR is activated by IP_3R-mediated Ca^{2+} release, in a signaling process
359 that has been termed Calcium-Induced Calcium Release (CICR) (Berridge, 1998). Since IP_3Rs
360 and RyRs have been placed together in CICR signaling processes in other systems, we wished
361 to test if IP_3 signaling and RyR functions might support the maintenance of PHP at the Drosophila
362 NMJ via a single signaling pathway. If this were the case, the expectation would be that a dual
363 block of PHP (consisting of IP_3 sequestration + RyR pharmacological blockade) would not de-
364 press quantal content below either individual manipulation.

365 The chronic *GluRIII[RNAi]*-expression condition is amenable both to pharmacology and
366 dual-tissue (*Pre-* + *Post-Gal4*) *UAS-IP$_3$-sponge* expression. As expected from before (Figs. 2, 5),
367 both 10 μM Dantrolene application on *GluRIII[RNAi]* NMJs and *UAS-IP$_3$-sponge* expression in a
368 *GluRIII[RNAi]* background blocked the long-term maintenance of PHP (Figs. 5D, E). This resulted
369 in evoked EPSP events that were blunted compared to *GluRIII[RNAi]* alone controls (Fig. 5E).
370 Interestingly, when we combined dantrolene application and *UAS-IP$_3$-sponge* expression in the
371 *GluRIII[RNAi]* background, the PHP impairment was indistinguishable from the impairment elic-
372 ited by Dantrolene alone or *UAS-IP$_3$-sponge* alone (Figs. 5D, E). These data are consistent with
373 a model in which IP_3 sequestration and RyR blockade disrupt the long-term maintenance of PHP
374 as part of a shared pathway (Fig. 5D).

375

376 **Neuron and muscle IP_3 signaling both contribute to long-term homeostatic potentiation**

377 Insofar, none of the genetic or pharmacological manipulations impairing PHP in this study
378 have been tissue specific. In principle, all PHP-blocking manipulations described could operate
379 either in neuronal or muscle substrates – or upon both tissues. Our prior work showed that chronic
380 *Plc21C* gene knockdown in the muscle alone is not sufficient to impair PHP (Brusich et al., 2015).
381 Taken alone, this result suggests a neuronal component to this signaling system for PHP mainte-
382 nance. Further experiments are needed to draw conclusions. We wished to understand whether
383 a pre- or postsynaptic mechanism (or a dual-tissue mechanism) governs the Ca^{2+} store release
384 signaling in order to support long-term maintenance of PHP.

385 We turned to the *UAS-IP$_3$-sponge* transgene because it can be expressed in a tissue-
386 specific manner, and it conveyed a full block of PHP when dually expressed in the neuron and
387 muscle (Fig. 2). We expressed *UAS-IP$_3$-sponge* in a *Gal4* driver control (neuron or muscle alone)
388 or a driver + *GluRIIA^{SP16}* null genetic background. We then quantified PHP by NMJ electrophysi-
389 ology, considering neuronal (Fig. 6A) or muscle (Fig. 6B) expression (Supplementary Table S5
390 for Fig. 6 electrophysiology data). Surprisingly, for both tissues alone, there was an small increase
391 in QC in a *UAS-IP$_3$-sponge* + *GluRIIA^{SP16}* genetic condition, compared to control *UAS-IP$_3$-sponge*
392 expression in an unchallenged background (Figs. 6A, B). Even though there was partial QC com-
393 pensation, evoked EPSP values were depressed versus controls when *UAS-IP$_3$-sponge* was ex-
394 pressed neuronally (Fig. 6C). Combined with our prior data (Fig. 2), we conclude that the mainte-
395 nance of PHP can only be fully erased with a dual-tissue inhibition of IP_3 signaling (Fig. 7).
396 Our data indicate that IP_3 functions in a pathway with Ca^{2+} store release (Fig. 5). Presyn-
397 aptic neurotransmitter release at the NMJ and other synapses is highly sensitive to changes in
398 intracellular Ca^{2+} concentration after influx through voltage-gated Ca_V2 channels. Therefore, we
399 needed to check if IP_3 signaling and its effects on intracellular Ca^{2+} release might impinge upon
400 the Ca^{2+} sensing machinery in the presynaptic cleft, which could potentially influence PHP. We
401 conducted additional NMJ recordings over a range of low extracellular [Ca^{2+}] (0.2-0.5 mM) and
402 calculated the Ca^{2+} cooperativity of release for the dual-tissue expression *UAS-IP$_3$-sponge* NMJs,
403 as well as wild-type NMJs and GAL4 driver control NMJs. The Ca^{2+} cooperativity of release re-
404 mained unchanged between the three conditions (Fig. 6D), indicating that sequestration of cellular
405 IP_3 at the NMJ does not directly alter the Ca^{2+}-dependence of synaptic release at the presynaptic
406 NMJ.
407
408

409 **DISCUSSION**

410 We divide expression of a homeostatic signaling paradigm into acute induction and
411 chronic maintenance stages. Two factors that govern the expression of these stages of PHP are
412 the nature of an NMJ synaptic challenge and the amount of time elapsed after presentation of the
413 challenge. Acute pharmacological inhibition of postsynaptic glutamate receptors initiates a rapid
414 induction of PHP that restores synaptic output in minutes (Frank et al., 2006). By contrast, genetic
415 lesions and other long-term reductions of NMJ sensitivity to neurotransmitter induce PHP in a way
416 that is sustained throughout life (Brusich et al., 2015; Davis et al., 1998; DiAntonio et al., 1999;
417 Paradis et al., 2001; Petersen et al., 1997). Our study has two core findings. The first is that the
418 short-term induction and long-term maintenance of PHP are separable by genetic and pharma-
419 cological manipulations. The second is that an IP_3-mediated signaling system is specifically re-
420 quired for the maintenance of PHP.

421

422 **Acute Versus Chronic PHP Expression**

423 For several years, one assumption has been that both the acute and chronic forms of PHP
424 are executed in a similar way – and possibly by shared mechanisms. The issue has been clouded
425 by the fact that both PhTox and a *GluRIIA* deletion mutant – the primary reagents utilized to induce
426 PHP – have the same molecular target, i.e. GluRIIA-containing glutamate receptors (Frank et al.,
427 2006; Petersen et al., 1997). The process of combining these acute and chronic forms of plasticity
428 within a single genotypic background was cumbersome due to a lack of reagents available to
429 conduct temporally separate targeting experiments.

430 Some insights into temporal requirements have been ascertained by testing potential ho-
431 meostatic signaling genes these two reagents, PhTox and *GluRIIA* mutant. The main finding has
432 been that the majority of molecules identified are essential to both the acute and chronic forms of
433 PHP (Davis and Müller, 2015; Frank, 2014a). Neurons tightly control neurotransmitter release
434 probability, and the core presynaptic machinery directly responsible for increasing quantal content
435 is shared. These shared components include the Ca_V2-type voltage-gated calcium channel or

436 factors gating influx through the channel (Frank et al., 2006; Frank et al., 2009; Müller and Davis,
437 2012; Wang et al., 2014; Wang et al., 2016a; Younger et al., 2013). They also include factors that
438 regulate the size of the readily releasable pool (RRP) of presynaptic vesicles (Harris et al., 2015;
439 Müller et al., 2015; Müller et al., 2012; Wang et al., 2016a; Weyhersmüller et al., 2011) or factors
440 that control the baseline excitability of the presynaptic motor neuron (Bergquist et al., 2010; Orr
441 et al., 2017b; Parrish et al., 2014; Younger et al., 2013) – and neurotransmitter fusion events
442 themselves (Dickman and Davis, 2009; Dickman et al., 2012; Müller et al., 2011). As a result,
443 both the acute and chronic forms of PHP signaling cause increases in readily releasable pool
444 (RRP) size and Ca_V2-mediated calcium influx; and in turn, these presynaptic mechanisms under-
445 lie the increases in QC which constitute PHP (Davis and Müller, 2015; Müller and Davis, 2012;
446 Müller et al., 2012).

447 Here we show that although the acute and chronic processes might largely overlap, they
448 are functionally distinct. The fact that the short-term induction of PHP and the long-term mainte-
449 nance of PHP are separable is not necessarily surprising. This finding is consistent with a growing
450 body of work showing that discrete genetic manipulations that only block a chronic implementation
451 of PHP. Collectively, the data indicate that the rapid induction of PHP uses a subset of the mole-
452 cules required to sustain PHP. Surprisingly, both sides of the synapse express molecules dispen-
453 sable for the rapid induction of HSP. Some of the proteins specifically required to sustain PHP
454 include neuronal factors like the Rho-type guanine exchange factor Ephexin (Frank et al., 2009),
455 as well as the transcription factor Gooseberry (Marie et al., 2010) and muscle-specific factors like
456 C-terminal Src kinase and Src family kinase members (Spring et al., 2016), as well as Target of
457 Rapamycin (Tor) and its effector molecules (Goel et al., 2017; Kauwe et al., 2016; Penney et al.,
458 2012). We have added PLCβ (Brusich et al., 2015) and its effectors IP_3R and RyR to the list of
459 molecules required only for sustaining PHP.

460 A new series of studies have augmented the idea of overlapping signaling pathways and
461 added a degree of specificity. Recent data suggest that both acute and chronic forms of PHP

462 begin as instructive retrograde signals in the muscle (Orr et al., 2017a), involve decrease in phos-
463 phorylation of muscle CaMKII levels, and converge upon the same signaling components in the
464 presynaptic neuron (Goel et al., 2017; Li et al., 2018; Newman et al., 2017). These experiments
465 also show that Tor converges on the same molecular targets as acute forms of PHP (Goel et al.,
466 2017). However, the precise roles for Tor and CamKII in either form of PHP are as yet unknown.
467

468 **PHP Stage Separation**

469 Our new data delineating a separation of the short-term induction of a homeostatic signal-
470 ing process and its long-term maintenance appear to contradict the idea of PHP pathway conver-
471 gence. Yet our findings are not necessarily contradictory to the published studies. Multiple lines
472 of evidence indicate discrete signaling requirements for acute forms of PHP on both sides of the
473 synapse. Although it is inferred that there is a single synaptic point of convergence (Goel et al.,
474 2017), this postsynaptic (or presynaptic) mechanistic convergence point is undefined. Accounting
475 for the separation of acute and chronic forms of PHP, as well as their discrete signaling require-
476 ments, these might require more than a single convergence point – or it might indicate that long-
477 term maintenance of PHP might actually integrate multiple signals between the muscle and neu-
478 ron over time. It will be important to clearly define roles of signaling systems underlying PHP in
479 future studies – and how distinct signaling systems might be linked.

480 Our work presents two unexpected findings. The first is that even in the face of a chronic
481 block of homeostatic potentiation, the NMJ is nevertheless capable of a rapid induction (Fig. 2F).
482 Given that most molecules identified to date are required for both phases, we did not expect
483 significant functional separation between the phases. Instead, we had expected *a priori* that a
484 failure of the chronic maintenance of PHP would make core machinery unavailable for its acute
485 induction. Despite increasing quantal content, evoked event amplitude was only restored to inter-
486 mediate levels seen in non-PhTox treated synapses rather than wild type levels. These findings
487 point to a failure to properly integrate information from PHP maintenance and induction pathways.

488 The second unexpected finding is how quickly the chronic maintenance of PHP can be
489 nullified by pharmacology (10 min), resulting in a return to baseline neurotransmitter release prob-
490 ability after only minutes of drug exposure (Figs. 4,5). Specifically, in this study, we showed that
491 homeostatic potentiation in *GluRIIA* mutant larvae or *GluRIII* knock-down larvae was abrogated
492 by four different reagents previously known to block RyR (Fig. 5) or IP_3R (Fig. 4), and quantal
493 content remained to levels seen in drug-treated wild-type larvae. That finding is reminiscent of
494 prior work showing that acute blockade of DAG/ENaC channels with the drug benzamil abolishes
495 PHP in both a *GluRIIA* mutant background, as well as in the presence of PhTox (Younger et al.,
496 2013). Yet the difference between benzamil application and the pharmacological agents used in
497 our study is that the drugs we employed only abolished PHP in a chronically challenged back-
498 ground. Together, these studies show that chronically expressed PHP does not alter baseline
499 neurotransmission properties. Rather it supplements baseline neurotransmission levels. This in-
500 dicates that the sustained expression of PHP likely continuously adjusts neurotransmission re-
501 lease independent of mechanisms which set baseline parameters.
502
503 **PLCβ- and IP_3-directed Signaling is Required for PHP Maintenance**
504 Our data strongly suggest that intracellular calcium channel activation and store release
505 fine tune neurotransmitter release that is implemented by PHP. The exact mechanism by which
506 IP_3R and RyR function to maintain PHP at the NMJ is unclear. It appears to be a shared pathway
507 with IP_3 (Fig. 5). If these store-release channels are acting downstream of IP_3 activity, then our
508 data suggest that this would be a coordinated activity involving both the muscle and the neuron
509 (Figs. 6, 7) – with loss of IP_3 signaling in the neuron being more detrimental to evoked release
510 (Fig. 6C).
511 Interestingly, both RyR and IP_3R have previously been shown to be critical for specific
512 aspects of neuroplasticity and neurotransmission (Berridge, 2016). Moreover, both activities of
513 both RyR and IP_3R can activate neuronal molecules that drive plasticity, such as calcineurin

514 (Victor et al., 1995) and CaMKII (Shakiryanova et al., 2011). By ways of example, at rodent hip-
515 pocampal synapses, properties like paired pulse facilitation, frequency of spontaneous neuro-
516 transmitter release (Emptage et al., 2001) are all modulated by RyR and/or IP_3R function, as is
517 facilitation of evoked neurotransmitter at the rat neocortex (Mathew and Hablitz, 2008). In addition
518 to vesicle fusion apparatus, activity of presynaptic voltage gated calcium channels is modulated
519 by intracellular calcium (Catterall, 2011; Lee et al., 2000).

520 Within the presynaptic neuron, IP_3R and RyR could activate any number of calcium-de-
521 pendent molecules to propagate homeostatic signaling. We directly tested some candidates in
522 our screen (Fig. 2, Supplementary Table S2), and none of those discrete tests blocked PHP. One
523 possibility is that the reagents we utilized did not sufficiently diminish the function of target mole-
524 cules enough to impact PHP in this directed screen. Another possibility is that calcium release via
525 IP_3R and RyR may directly potentiate neurotransmitter release, either by potentiating basal cal-
526 cium levels or synchronously with Ca_V2-type voltage gated calcium channels (Frank et al., 2006;
527 Müller and Davis, 2012).

528 Both pre- and postsynaptic voltage-gated calcium channels are critical for the expression
529 of several forms of homeostatic synaptic plasticity (Frank, 2014b). Much evidence supports the
530 hypothesis that store-operated channels and voltage gated calcium channels interact to facilitate
531 PHP. In various neuronal populations, both RyR and IP_3R interact with L-type calcium channels
532 physically and functionally to reciprocally impact the opening of the other channel (Chavis et al.,
533 1996; Kim et al., 2007; Ouardouz et al., 2003). In presynaptic boutons, RyR calcium release fol-
534 lows action potential firing (Emptage et al., 2001). Calcium imaging experiments show that both
535 the acute expression and sustained maintenance of PHP requires an increase in presynaptic
536 calcium following an action potential (Müller and Davis, 2012). Because IP_3Rs are activated by
537 both free calcium and IP_3, elevated IP_3 levels in the case of chronically expressed PHP could
538 allow IP_3Rs and RyRs to open in a way that is time-locked with Ca_V2-mediated calcium influx or
539 in a way to facilitate the results of later Ca_V2-mediated influx.

540

ACKNOWLEDGEMENTS

We thank members of the Frank lab for helpful comments on earlier versions of this study, and the laboratories of Drs. Tina Tootle, Fang Lin, Toshihiro Kitamoto, Pamela Geyer, and Lori Wallrath for helpful discussions. We also thank Drs. Andrew Russo, N. Charles Harata, and Christopher Ahern for helpful suggestions. We thank the Bloomington Drosophila Stock Center and the Vienna Drosophila Resource Center for several fly stocks detailed in the Materials and Methods Section and Supplementary Tables.

548 **REFERENCES**

549

550 Andersen, N., Krauth, N., and Nabavi, S. (2017). Hebbian plasticity in vivo: relevance and
551 induction. Curr Opin Neurobiol *45*, 188-192.

552 Bergquist, S., Dickman, D.K., and Davis, G.W. (2010). A hierarchy of cell intrinsic and target-
553 derived homeostatic signaling. Neuron *66*, 220-234.

554 Berridge, M.J. (1984). Inositol trisphosphate and diacylglycerol as second messengers.
555 Biochem J *220*, 345-360.

556 Berridge, M.J. (1987). Inositol trisphosphate and diacylglycerol: two interacting second
557 messengers. Annu Rev Biochem *56*, 159-193.

558 Berridge, M.J. (1998). Neuronal calcium signaling. Neuron *21*, 13-26.

559 Berridge, M.J. (2016). The Inositol Trisphosphate/Calcium Signaling Pathway in Health and
560 Disease. Physiol Rev *96*, 1261-1296.

561 Bootman, M.D., Collins, T.J., Mackenzie, L., Roderick, H.L., Berridge, M.J., and Peppiatt, C.M.
562 (2002). 2-aminoethoxydiphenyl borate (2-APB) is a reliable blocker of store-operated Ca2+
563 entry but an inconsistent inhibitor of InsP3-induced Ca2+ release. FASEB journal : official
564 publication of the Federation of American Societies for Experimental Biology *16*, 1145-1150.

565 Brusich, D.J., Spring, A.M., and Frank, C.A. (2015). A single-cross, RNA interference-based
566 genetic tool for examining the long-term maintenance of homeostatic plasticity. Frontiers in
567 cellular neuroscience *9*, 107.

568 Budnik, V., Koh, Y.H., Guan, B., Hartmann, B., Hough, C., Woods, D., and Gorczyca, M. (1996).
569 Regulation of synapse structure and function by the Drosophila tumor suppressor gene dlg.
570 Neuron *17*, 627-640.

571 Castonguay, A., and Robitaille, R. (2002). Xestospongin C is a potent inhibitor of SERCA at a
572 vertebrate synapse. Cell Calcium *32*, 39-47.

573 Catterall, W.A. (2011). Voltage-gated calcium channels. Cold Spring Harb Perspect Biol *3*,
574 a003947.

575 Chavis, P., Fagni, L., Lansman, J.B., and Bockaert, J. (1996). Functional coupling between
576 ryanodine receptors and L-type calcium channels in neurons. Nature *382*, 719-722.

577 Chen, X., and Dickman, D. (2017). Development of a tissue-specific ribosome profiling
578 approach in Drosophila enables genome-wide evaluation of translational adaptations. PLoS
579 genetics *13*, e1007117.

580 Cremona, O., and De Camilli, P. (2001). Phosphoinositides in membrane traffic at the synapse.
581 Journal of cell science *114*, 1041-1052.

582 Cull-Candy, S.G., Miledi, R., Trautmann, A., and Uchitel, O.D. (1980). On the release of
583 transmitter at normal, myasthenia gravis and myasthenic syndrome affected human end-plates.
584 J Physiol *299*, 621-638.

585 Davis, G.W. (2006). Homeostatic control of neural activity: from phenomenology to molecular
586 design. Annu Rev Neurosci *29*, 307-323.

587 Davis, G.W., DiAntonio, A., Petersen, S.A., and Goodman, C.S. (1998). Postsynaptic PKA
588 controls quantal size and reveals a retrograde signal that regulates presynaptic transmitter
589 release in Drosophila. Neuron *20*, 305-315.

590 Davis, G.W., and Müller, M. (2015). Homeostatic control of presynaptic neurotransmitter
591 release. Annu Rev Physiol *77*, 251-270.

592 DiAntonio, A., Petersen, S.A., Heckmann, M., and Goodman, C.S. (1999). Glutamate receptor
593 expression regulates quantal size and quantal content at the Drosophila neuromuscular
594 junction. J Neurosci *19*, 3023-3032.

595 Dickman, D.K., and Davis, G.W. (2009). The schizophrenia susceptibility gene dysbindin
596 controls synaptic homeostasis. Science *326*, 1127-1130.

597 Dickman, D.K., Tong, A., and Davis, G.W. (2012). Snapin is critical for presynaptic homeostatic
598 plasticity. J Neurosci *32*, 8716-8724.

599 Dietzl, G., Chen, D., Schnorrer, F., Su, K.C., Barinova, Y., Fellner, M., Gasser, B., Kinsey, K.,
600 Oppel, S., Scheiblauer, S.*, et al.* (2007). A genome-wide transgenic RNAi library for conditional
601 gene inactivation in Drosophila. Nature *448*, 151-156.

602 Diver, J.M., Sage, S.O., and Rosado, J.A. (2001). The inositol trisphosphate receptor antagonist
603 2-aminoethoxydiphenylborate (2-APB) blocks Ca2+ entry channels in human platelets: cautions
604 for its use in studying Ca2+ influx. Cell calcium *30*, 323-329.

605 Emptage, N.J., Reid, C.A., and Fine, A. (2001). Calcium stores in hippocampal synaptic boutons
606 mediate short-term plasticity, store-operated Ca2+ entry, and spontaneous transmitter release.
607 Neuron *29*, 197-208.

608 Frank, C.A. (2014a). Homeostatic plasticity at the Drosophila neuromuscular junction.
609 Neuropharmacology *78*, 63-74.

610 Frank, C.A. (2014b). How voltage-gated calcium channels gate forms of homeostatic synaptic
611 plasticity. Frontiers in cellular neuroscience *8*, 40.

612 Frank, C.A., Kennedy, M.J., Goold, C.P., Marek, K.W., and Davis, G.W. (2006). Mechanisms
613 underlying the rapid induction and sustained expression of synaptic homeostasis. Neuron *52*,
614 663-677.

615 Frank, C.A., Pielage, J., and Davis, G.W. (2009). A presynaptic homeostatic signaling system
616 composed of the Eph receptor, ephexin, Cdc42, and CaV2.1 calcium channels. Neuron *61*, 556-
617 569.

618 Gafni, J., Munsch, J.A., Lam, T.H., Catlin, M.C., Costa, L.G., Molinski, T.F., and Pessah, I.N.
619 (1997). Xestospongins: potent membrane permeable blockers of the inositol 1,4,5-trisphosphate
620 receptor. Neuron *19*, 723-733.

621 Genç, Ö., Dickman, D.K., Ma, W., Tong, A., Fetter, R.D., and Davis, G.W. (2017). MCTP is an
622 ER-resident calcium sensor that stabilizes synaptic transmission and homeostatic plasticity.
623 eLife *6*.

624 Goel, P., Li, X., and Dickman, D. (2017). Disparate Postsynaptic Induction Mechanisms
625 Ultimately Converge to Drive the Retrograde Enhancement of Presynaptic Efficacy. Cell reports
626 *21*, 2339-2347.

627 Goni, F.M., and Alonso, A. (1999). Structure and functional properties of diacylglycerols in
628 membranes. Progress in lipid research *38*, 1-48.

629 Greenspan, R.J. (2004). Fly pushing : the theory and practice of Drosophila genetics, 2nd edn
630 (Cold Spring Harbor, N.Y.: Cold Spring Harbor Laboratory Press).

631 Harris, N., Braiser, D.J., Dickman, D.K., Fetter, R.D., Tong, A., and Davis, G.W. (2015). The
632 Innate Immune Receptor PGRP-LC Controls Presynaptic Homeostatic Plasticity. Neuron *88*,
633 1157-1164.

634 Hazelrigg, T., Levis, R., and Rubin, G.M. (1984). Transformation of white locus DNA in
635 drosophila: dosage compensation, zeste interaction, and position effects. Cell *36*, 469-481.

636 Huang, F.D., Woodruff, E., Mohrmann, R., and Broadie, K. (2006). Rolling blackout is required
637 for synaptic vesicle exocytosis. J Neurosci *26*, 2369-2379.

638 Kadamur, G., and Ross, E.M. (2012). Mammalian Phospholipase C. Annu Rev Physiol.

639 Kauwe, G., Tsurudome, K., Penney, J., Mori, M., Gray, L., Calderon, M.R., Elazouzzi, F.,
640 Chicoine, N., Sonenberg, N., and Haghighi, A.P. (2016). Acute Fasting Regulates Retrograde
641 Synaptic Enhancement through a 4E-BP-Dependent Mechanism. Neuron *92*, 1204-1212.

642 Kikuma, K., Li, X., Kim, D., Sutter, D., and Dickman, D.K. (2017). Extended Synaptotagmin
643 Localizes to Presynaptic ER and Promotes Neurotransmission and Synaptic Growth in
644 Drosophila. Genetics.

645 Kim, S., Yun, H.M., Baik, J.H., Chung, K.C., Nah, S.Y., and Rhim, H. (2007). Functional
646 interaction of neuronal Cav1.3 L-type calcium channel with ryanodine receptor type 2 in the rat
647 hippocampus. The Journal of biological chemistry *282*, 32877-32889.

648 Lee, A., Scheuer, T., and Catterall, W.A. (2000). Ca2+/calmodulin-dependent facilitation and
649 inactivation of P/Q-type Ca2+ channels. J Neurosci *20*, 6830-6838.

650 Li, X., Goel, P., Chen, C., Angajala, V., Chen, X., and Dickman, D.K. (2018). Synapse-specific
651 and compartmentalized expression of presynaptic homeostatic potentiation. eLife *7*.

652 Lin, D.M., and Goodman, C.S. (1994). Ectopic and increased expression of Fasciclin II alters
653 motoneuron growth cone guidance. Neuron *13*, 507-523.

654 Lisman, J., Yasuda, R., and Raghavachari, S. (2012). Mechanisms of CaMKII action in long-
655 term potentiation. Nat Rev Neurosci *13*, 169-182.

656 Marie, B., Pym, E., Bergquist, S., and Davis, G.W. (2010). Synaptic homeostasis is consolidated
657 by the cell fate gene gooseberry, a Drosophila pax3/7 homolog. J Neurosci *30*, 8071-8082.

658 Martin, A.R. (1955). A further study of the statistical composition on the end-plate potential. J
659 Physiol *130*, 114-122.

660 Maruyama, T., Kanaji, T., Nakade, S., Kanno, T., and Mikoshiba, K. (1997). 2APB, 2-
661 aminoethoxydiphenyl borate, a membrane-penetrable modulator of Ins(1,4,5)P3-induced Ca2+
662 release. J Biochem *122*, 498-505.

663 Mathew, S.S., and Hablitz, J.J. (2008). Calcium release via activation of presynaptic IP3
664 receptors contributes to kainate-induced IPSC facilitation in rat neocortex. Neuropharmacology
665 *55*, 106-116.

666 Müller, M., and Davis, G.W. (2012). Transsynaptic control of presynaptic Ca(2)(+) influx
667 achieves homeostatic potentiation of neurotransmitter release. Curr Biol *22*, 1102-1108.

668 Müller, M., Genç, Ö., and Davis, G.W. (2015). RIM-Binding Protein Links Synaptic Homeostasis
669 to the Stabilization and Replenishment of High Release Probability Vesicles. Neuron *85*, 1056-
670 1069.

671 Müller, M., Liu, K.S., Sigrist, S.J., and Davis, G.W. (2012). RIM Controls Homeostatic Plasticity
672 through Modulation of the Readily-Releasable Vesicle Pool. J Neurosci *32*, 16574-16585.

673 Müller, M., Pym, E.C., Tong, A., and Davis, G.W. (2011). Rab3-GAP controls the progression of
674 synaptic homeostasis at a late stage of vesicle release. Neuron *69*, 749-762.

675 Murmu, M.S., Stinnakre, J., and Martin, J.R. (2010). Presynaptic Ca2+ stores contribute to odor-
676 induced responses in Drosophila olfactory receptor neurons. J Exp Biol *213*, 4163-4173.

677 Newman, Z.L., Hoagland, A., Aghi, K., Worden, K., Levy, S.L., Son, J.H., Lee, L.P., and Isacoff,
678 E.Y. (2017). Input-Specific Plasticity and Homeostasis at the Drosophila Larval Neuromuscular
679 Junction. Neuron *93*, 1388-1404 e1310.

680 Ni, J.Q., Liu, L.P., Binari, R., Hardy, R., Shim, H.S., Cavallaro, A., Booker, M., Pfeiffer, B.D.,
681 Markstein, M., Wang, H.*, et al.* (2009). A Drosophila resource of transgenic RNAi lines for
682 neurogenetics. Genetics *182*, 1089-1100.

683 O'Brien, R.J., Kamboj, S., Ehlers, M.D., Rosen, K.R., Fischbach, G.D., and Huganir, R.L.
684 (1998). Activity-dependent modulation of synaptic AMPA receptor accumulation. Neuron *21*,
685 1067-1078.

686 Orr, B.O., Fetter, R.D., and Davis, G.W. (2017a). Retrograde semaphorin-plexin signalling
687 drives homeostatic synaptic plasticity. Nature *550*, 109-113.

688 Orr, B.O., Gorczyca, D., Younger, M.A., Jan, L.Y., Jan, Y.N., and Davis, G.W. (2017b).
689 Composition and Control of a Deg/ENaC Channel during Presynaptic Homeostatic Plasticity.
690 Cell reports *20*, 1855-1866.

691 Ouardouz, M., Nikolaeva, M.A., Coderre, E., Zamponi, G.W., McRory, J.E., Trapp, B.D., Yin, X.,
692 Wang, W., Woulfe, J., and Stys, P.K. (2003). Depolarization-induced Ca2+ release in ischemic
693 spinal cord white matter involves L-type Ca2+ channel activation of ryanodine receptors.
694 Neuron *40*, 53-63.

695 Paradis, S., Sweeney, S.T., and Davis, G.W. (2001). Homeostatic control of presynaptic release
696 is triggered by postsynaptic membrane depolarization. Neuron *30*, 737-749.

697 Parrish, J.Z., Kim, C.C., Tang, L., Bergquist, S., Wang, T., Derisi, J.L., Jan, L.Y., Jan, Y.N., and
698 Davis, G.W. (2014). Kruppel mediates the selective rebalancing of ion channel expression.
699 Neuron *82*, 537-544.

700 Penney, J., Tsurudome, K., Liao, E.H., Elazzouzi, F., Livingstone, M., Gonzalez, M., Sonenberg,
701 N., and Haghighi, A.P. (2012). TOR is required for the retrograde regulation of synaptic
702 homeostasis at the Drosophila neuromuscular junction. Neuron *74*, 166-178.

703 Peters, C., Bayer, M.J., Buhler, S., Andersen, J.S., Mann, M., and Mayer, A. (2001). Trans-
704 complex formation by proteolipid channels in the terminal phase of membrane fusion. Nature
705 *409*, 581-588.

706 Petersen, S.A., Fetter, R.D., Noordermeer, J.N., Goodman, C.S., and DiAntonio, A. (1997).
707 Genetic analysis of glutamate receptors in Drosophila reveals a retrograde signal regulating
708 presynaptic transmitter release. Neuron *19*, 1237-1248.

709 Philip, F., Kadamur, G., Silos, R.G., Woodson, J., and Ross, E.M. (2010). Synergistic activation
710 of phospholipase C-beta3 by Galpha(q) and Gbetagamma describes a simple two-state
711 coincidence detector. Curr Biol *20*, 1327-1335.

712 Plomp, J.J., van Kempen, G.T., and Molenaar, P.C. (1992). Adaptation of quantal content to
713 decreased postsynaptic sensitivity at single endplates in alpha-bungarotoxin-treated rats. J
714 Physiol *458*, 487-499.

715 Poo, M.M., Pignatelli, M., Ryan, T.J., Tonegawa, S., Bonhoeffer, T., Martin, K.C., Rudenko, A.,
716 Tsai, L.H., Tsien, R.W., Fishell, G.*, et al.* (2016). What is memory? The present state of the
717 engram. BMC Biol *14*, 40.

718 Pozo, K., and Goda, Y. (2010). Unraveling mechanisms of homeostatic synaptic plasticity.
719 Neuron *66*, 337-351.

720 Rohrbough, J., and Broadie, K. (2005). Lipid regulation of the synaptic vesicle cycle. Nat Rev
721 Neurosci *6*, 139-150.

722 Russell, J.F., Fu, Y.H., and Ptacek, L.J. (2013). Episodic neurologic disorders: syndromes,
723 genes, and mechanisms. Annu Rev Neurosci *36*, 25-50.

724 Santulli, G., and Marks, A.R. (2015). Essential Roles of Intracellular Calcium Release Channels
725 in Muscle, Brain, Metabolism, and Aging. Curr Mol Pharmacol *8*, 206-222.

726 Santulli, G., Nakashima, R., Yuan, Q., and Marks, A.R. (2017). Intracellular calcium release
727 channels: an update. J Physiol *595*, 3041-3051.

728 Shakiryanova, D., Morimoto, T., Zhou, C., Chouhan, A.K., Sigrist, S.J., Nose, A., Macleod, G.T.,
729 Deitcher, D.L., and Levitan, E.S. (2011). Differential control of presynaptic CaMKII activation
730 and translocation to active zones. The Journal of neuroscience : the official journal of the
731 Society for Neuroscience *31*, 9093-9100.

732 Shortridge, R.D., Yoon, J., Lending, C.R., Bloomquist, B.T., Perdew, M.H., and Pak, W.L.
733 (1991). A Drosophila phospholipase C gene that is expressed in the central nervous system. J
734 Biol Chem *266*, 12474-12480.

735 Simkus, C.R., and Stricker, C. (2002). The contribution of intracellular calcium stores to
736 mEPSCs recorded in layer II neurones of rat barrel cortex. J Physiol *545*, 521-535.

737 Spring, A.M., Brusich, D.J., and Frank, C.A. (2016). C-terminal Src Kinase Gates Homeostatic
738 Synaptic Plasticity and Regulates Fasciclin II Expression at the Drosophila Neuromuscular
739 Junction. PLoS genetics *12*, e1005886.

740 Stewart, B.A., Atwood, H.L., Renger, J.J., Wang, J., and Wu, C.F. (1994). Improved stability of
741 Drosophila larval neuromuscular preparations in haemolymph-like physiological solutions.
742 Journal of comparative physiology A, Sensory, neural, and behavioral physiology *175*, 179-191.

743 Summerville, J.B., Faust, J.F., Fan, E., Pendin, D., Daga, A., Formella, J., Stern, M., and
744 McNew, J.A. (2016). The effects of ER morphology on synaptic structure and function in
745 Drosophila melanogaster. Journal of cell science *129*, 1635-1648.

746 Sutton, M.A., Ito, H.T., Cressy, P., Kempf, C., Woo, J.C., and Schuman, E.M. (2006). Miniature
747 neurotransmission stabilizes synaptic function via tonic suppression of local dendritic protein
748 synthesis. Cell *125*, 785-799.

749 Tedford, H.W., and Zamponi, G.W. (2006). Direct G protein modulation of Cav2 calcium
750 channels. Pharmacol Rev *58*, 837-862.

751 Turrigiano, G.G. (2017). The dialectic of Hebb and homeostasis. Philos Trans R Soc Lond B
752 Biol Sci *372*.

753 Turrigiano, G.G., Leslie, K.R., Desai, N.S., Rutherford, L.C., and Nelson, S.B. (1998). Activity-
754 dependent scaling of quantal amplitude in neocortical neurons. Nature *391*, 892-896.

755 Turrigiano, G.G., and Nelson, S.B. (2004). Homeostatic plasticity in the developing nervous
756 system. Nat Rev Neurosci *5*, 97-107.

757 Usui-Aoki, K., Matsumoto, K., Koganezawa, M., Kohatsu, S., Isono, K., Matsubayashi, H.,
758 Yamamoto, M.T., Ueda, R., Takahashi, K., Saigo, K.*, et al.* (2005). Targeted expression of Ip3
759 sponge and Ip3 dsRNA impaires sugar taste sensation in Drosophila. Journal of neurogenetics
760 *19*, 123-141.

761 Vazquez-Martinez, O., Canedo-Merino, R., Diaz-Munoz, M., and Riesgo-Escovar, J.R. (2003).
762 Biochemical characterization, distribution and phylogenetic analysis of Drosophila melanogaster
763 ryanodine and IP3 receptors, and thapsigargin-sensitive Ca2+ ATPase. Journal of cell science
764 *116*, 2483-2494.

765 Victor, R.G., Thomas, G.D., Marban, E., and O'Rourke, B. (1995). Presynaptic modulation of
766 cortical synaptic activity by calcineurin. Proceedings of the National Academy of Sciences of the
767 United States of America *92*, 6269-6273.

768 Wang, T., Hauswirth, A.G., Tong, A., Dickman, D.K., and Davis, G.W. (2014). Endostatin Is a
769 Trans-Synaptic Signal for Homeostatic Synaptic Plasticity. Neuron *83*, 616-629.

770 Wang, T., Jones, R.T., Whippen, J.M., and Davis, G.W. (2016a). alpha2delta-3 Is Required for
771 Rapid Transsynaptic Homeostatic Signaling. Cell reports *16*, 2875-2888.

772 Wang, X., Pinter, M.J., and Rich, M.M. (2016b). Reversible Recruitment of a Homeostatic
773 Reserve Pool of Synaptic Vesicles Underlies Rapid Homeostatic Plasticity of Quantal Content. J
774 Neurosci *36*, 828-836.

775 Weyhersmüller, A., Hallermann, S., Wagner, N., and Eilers, J. (2011). Rapid active zone
776 remodeling during synaptic plasticity. J Neurosci *31*, 6041-6052.

777 Wilcox, R.A., Primrose, W.U., Nahorski, S.R., and Challiss, R.A. (1998). New developments in
778 the molecular pharmacology of the myo-inositol 1,4,5-trisphosphate receptor. Trends Pharmacol
779 Sci *19*, 467-475.

780 Wu, L., Bauer, C.S., Zhen, X.G., Xie, C., and Yang, J. (2002). Dual regulation of voltage-gated
781 calcium channels by PtdIns(4,5)P2. Nature *419*, 947-952.

782 Xu, S.Z., Zeng, F., Boulay, G., Grimm, C., Harteneck, C., and Beech, D.J. (2005). Block of
783 TRPC5 channels by 2-aminoethoxydiphenyl borate: a differential, extracellular and voltage-
784 dependent effect. Br J Pharmacol *145*, 405-414.

785 Yeates, C.J., and Frank, C.A. (2017). Synaptic homeostasis at the Drosophila neuromuscular
786 junction is a reversible signaling process that is sensitive to high temperature (*bioRxiv*: doi:
787 https://doi.org/10.1101/154930).

788 Younger, M.A., Müller, M., Tong, A., Pym, E.C., and Davis, G.W. (2013). A presynaptic ENaC
789 channel drives homeostatic plasticity. Neuron *79*, 1183-1196.

790 Zhao, F., Li, P., Chen, S.R., Louis, C.F., and Fruen, B.R. (2001). Dantrolene inhibition of
791 ryanodine receptor Ca2+ release channels. Molecular mechanism and isoform selectivity. The
792 Journal of biological chemistry *276*, 13810-13816.

793

794

FIGURES, TABLES, AND LEGENDS

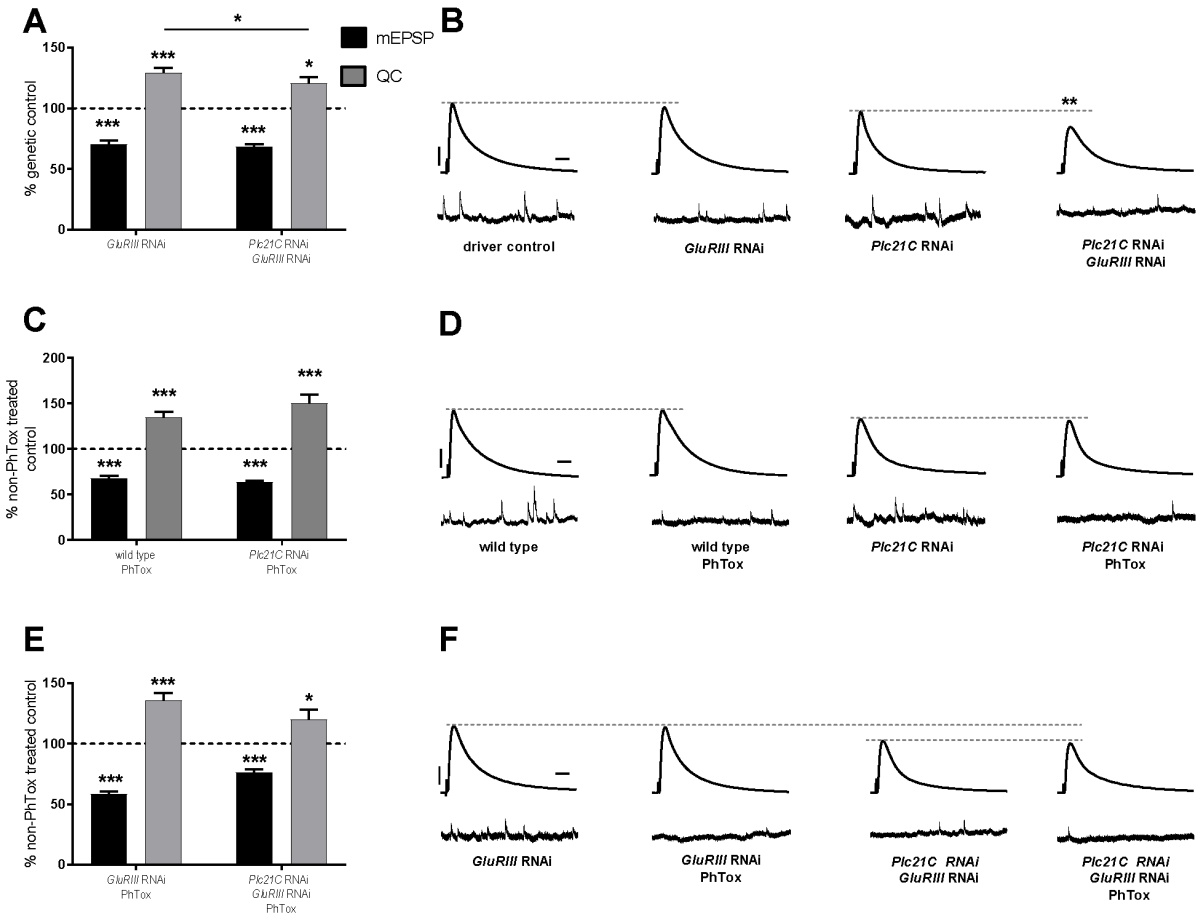

Figure 1: The maintenance of presynaptic homeostatic potentiation requires PLCβ, but the induction does not.

(A) *GluRIII* knockdown induces a significant decrease in quantal size and robust PHP (increase in quantal content) in response. This PHP response is partly impaired by concurrent *Plc21C* knockdown. **(B)** Representative electrophysiological traces of EPSPs (above) and mEPSPs (below). The evoked events show full PHP in the *GluRIII* RNAi knock down background, but only partial PHP with concurrent *Plc21C* knock down. **(C)** PHP is rapidly induced in wild-type and *Plc21C* RNAi larvae after a 10-minute incubation with 20 μM PhTox. Values are normalized to non-PhTox treated larvae of identical genotype. **(D)** Representative electrophysiological traces (as in (B)) showing intact PHP induction. **(E)** Dual activation of PHP maintenance and induction does not require PLCβ. mEPSP is further decreased and quantal content further increased in by PhTox treatment in *GluRIII* RNAi synapses compared to untreated synapses. Data on bar graphs are mean ± SEM. * $p < 0.05$, ** $p < 0.01$, *** $p < 0.001$ by Student's t-test versus non-challenged genetic control. Scale bars for all traces are y = 10 mV (1 mV), x = 20 ms (500 ms) for EPSPs (mEPSPs).

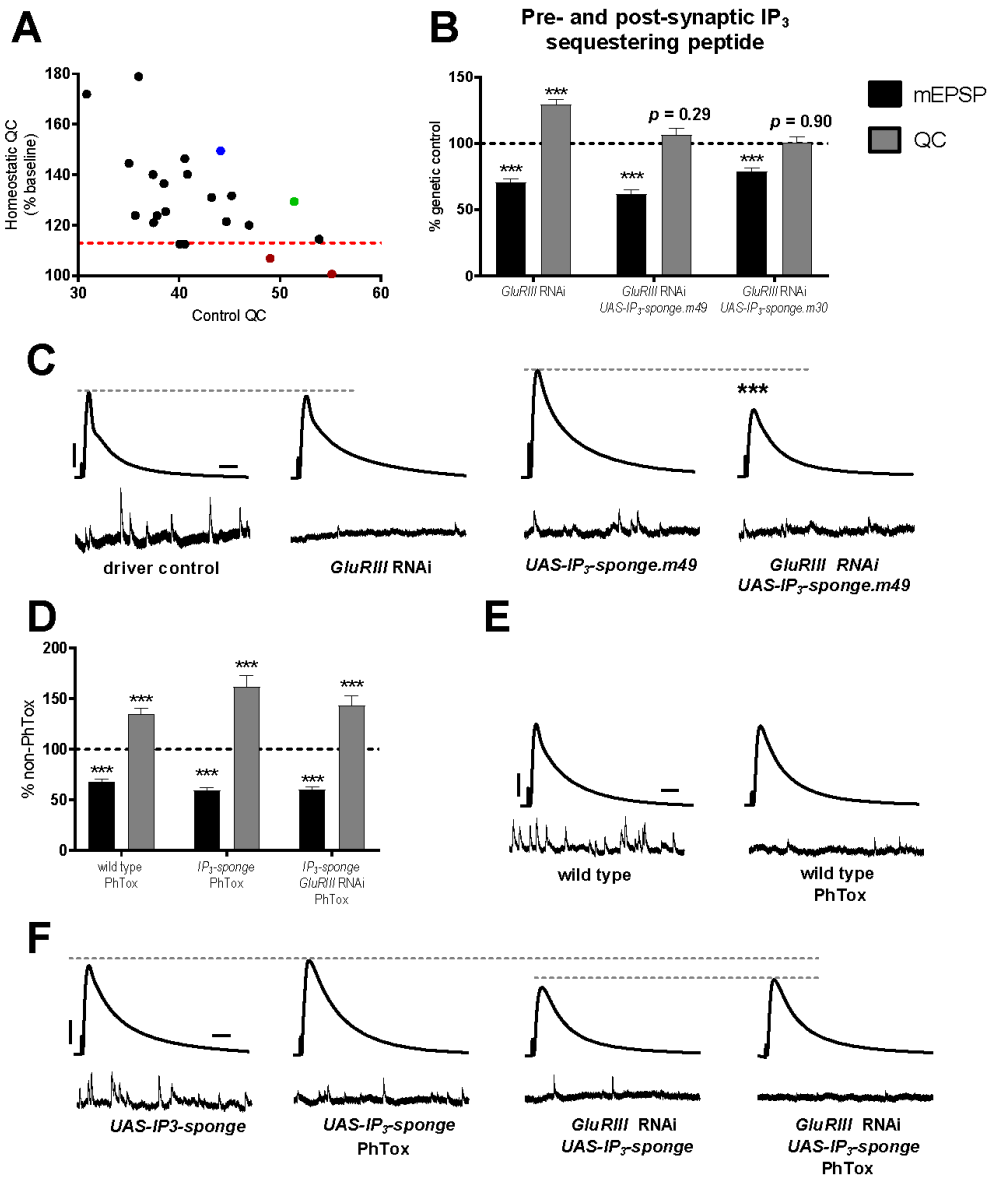

Figure 2: IP_3 sequestration blocks PHP maintenance but not PHP induction.

(A) Screen data, plotting baseline quantal content (QC, *x*-axis, genetic manipulation alone) versus QC of the homeostatically challenged condition (*y*-axis, *GluRIII RNAi* or *GluRIIA* mutant). Blue = *GluRIIA* alone. Green = *GluRIII* RNAi alone. Red = *GluRIII RNAi* + *UAS-IP_3-sponge.* Dotted line = one standard deviation below the mean QC of *GluRIII* RNAi. **(B)** Expression of either *UAS-IP_3-sponge* line resulted in a failure to sustain PHP. Values normalized to genetic control containing the same drivers and *UAS-IP_3-sponge* transgene but lacking the *GluRIII RNAi* construct. **(C)** Representative electrophysiological traces (EPSPs above; mEPSPs below), demonstrating significantly diminished evoked potentials in the *GluRIII RNAi* + *UAS-IP_3-sponge* condition due to a lack of PHP. **(D)** Failure to sustain PHP following IP_3 sequestration does not preclude its rapid induction. PhTox treatment results in significantly decreased mEPSP amplitude and a compensatory increase in QC. Bar graph values normalized to non-PhTox-treated controls of identical genotype. **(E)** Representative electrophysiological traces showing full homeostatic compensation with PhTox application (as in (Frank et al., 2006)). **(F)** Representative traces of the experimental data in (D). Data on bar graphs are mean ± SEM. * $p < 0.05$, ** $p < 0.01$, *** $p < 0.001$ by Student's t-test versus non-challenged genetic control. Scale bars for all traces are $y = 10$ mV (1 mV), $x = 20$ ms (500 ms) for EPSPs (mEPSPs).

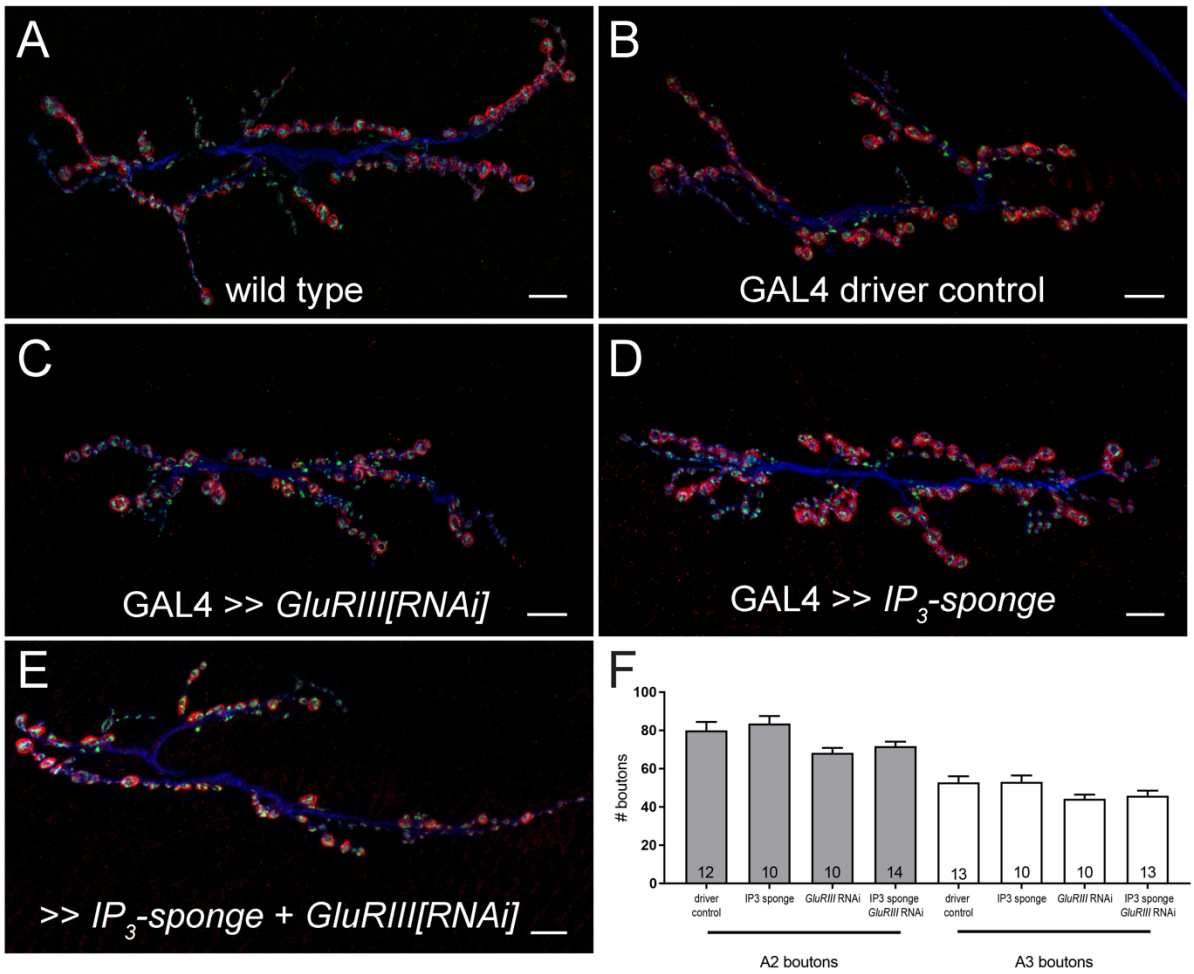

Figure 3: IP_3 sequestration does not impair NMJ growth

(A-E) NMJs were co-stained with anti-DLG (red) and anti-Synapsin antibodies (green) to visualize synaptic boutons, with anti-HRP (blue) to visualize presynaptic membranes. All scale bars, 10 μm. **(F)** NMJ growth was assessed by bouton counting at abdominal segments A2 and A3, muscle 6/7, based on postsynaptic DLG staining and double checked for presynaptic Synapsin. By bouton counts, no statistically significant difference in NMJ growth versus control was observed for any of the experimental conditions. Counts were compared for each segment using the Kruskal-Wallis ANOVA test followed by Dunn's multiple comparisons test. An overall difference in counts was detected for segment A2 ($p < 0.05$ for ANOVA), but no condition differed significantly from driver control (all $p > 0.1$ vs. control). No significant differences were detected for segment A3.

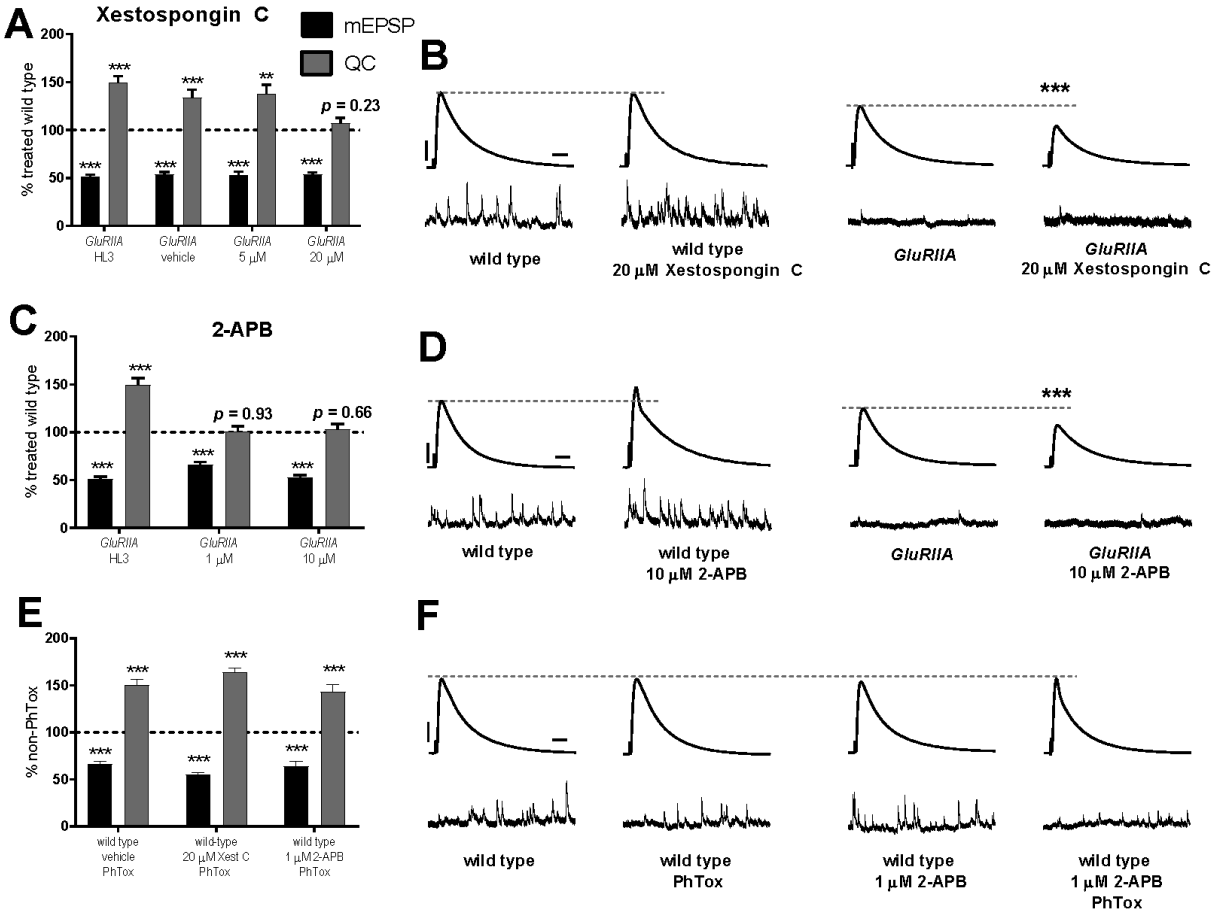

Figure 4: The maintenance of PHP requires continuous IP_3R function, but the induction does not.

(A) Acute NMJ application of Xestospongin C blocked PHP maintenance. Values normalized to identically treated, wild-type NMJ levels. Vehicle (DMSO) concentration equal to that used with 20 μM Xestospongin C. **(B)** Representative electrophysiological traces (EPSPs above; mEPSPs below) for conditions in (A). For 20 μM Xestospongin C application in a *GluRIIA* mutant background, EPSPs failed to achieve *GluRIIA* mutant NMJ levels because of a lack of sustained PHP. **(C)** Acute NMJ application of 2-APB application blocked PHP maintenance. Values normalized to identically treated, wild-type NMJ levels. Vehicle is DMSO, as in (A). **(D)** Representative electrophysiological traces (EPSPs above; mEPSPs below) for conditions in (C). For 10 μM 2-APB application in a *GluRIIA* mutant background, EPSPs failed to achieve *GluRIIA* mutant NMJ levels because of a lack of sustained PHP. **(E)** Acute induction of PHP following PhTox treatment was not blocked by Xestospongin C or 2-APB. Values normalized to otherwise identical controls, without PhTox. **(F)** Representative electrophysiological traces (EPSPs above; mEPSPs below) for conditions in (E). Data on bar graphs are mean ± SEM. * $p < 0.05$, ** $p < 0.01$, *** $p < 0.001$ by Student's t-test versus non-challenged genetic control. Scale bars for all traces are y = 10 mV (1 mV), x = 20 ms (500 ms) for EPSPs (mEPSPs).

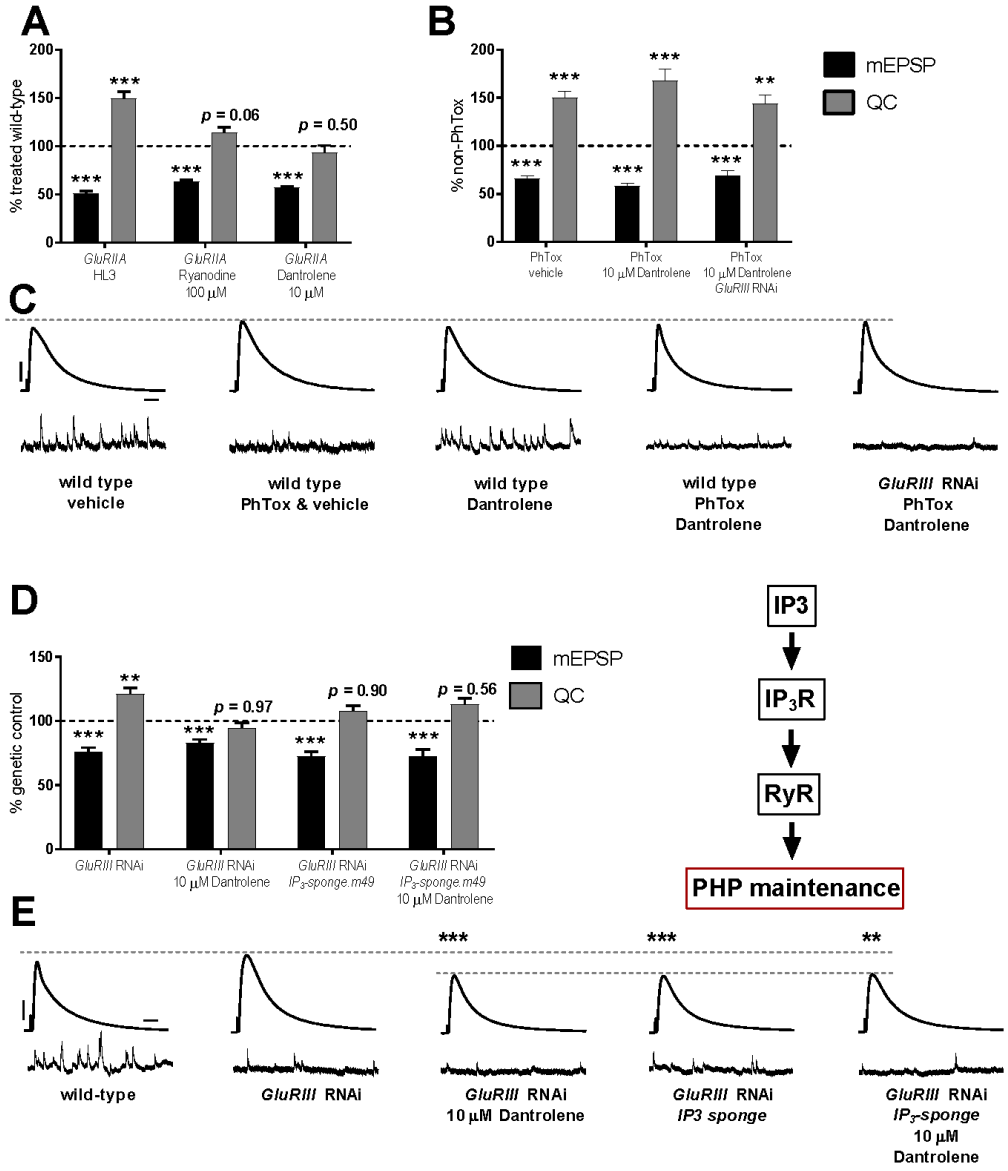

Figure 5: The maintenance of PHP requires continuous RyR function, but the induction does not.

(A) Acute NMJ application of either Ryanodine or Dantrolene blocked PHP maintenance. Values normalized to identically treated, wild-type NMJs. **(B)** By contrast, acute application of PhTox and Dantrolene left the acute induction of PHP intact. This acute induction of PHP was also intact in a *GluRIII* knockdown RNAi genetic background. Values normalized to levels identical genotypes without PhTox treatment. **(C)** Representative electrophysiological traces (EPSPs above; mEPSPs below) for the conditions in (B) showing intact PHP induction. **(D)** The molecular targets of Dantrolene and *IP_3-sponge* constitute a common pathway for the maintenance of PHP. Both treatments block PHP maintenance in a *GluRIII RNAi* genetic background but do not exert an additive effect. Values normalized to treated, non-*GluRIII* genetic control. **(E)** Representative electrophysiological traces for the conditions in (D). Data on bar graphs are mean ± SEM. QC analyzed by Student's t-Test vs. unchallenged controls (A, B) or across parallel conditions by one-way ANOVA followed by Bonferroni post-hoc test (D). mEPSP amplitude analyzed with Student's t-test versus treated, non-*GluRIII* genetic controls. * $p < 0.05$, ** $p < 0.01$, *** $p < 0.001$. Scale bars for all traces are y = 10 mV (1 mV), x = 20 ms (500 ms) for EPSPs (mEPSPs).

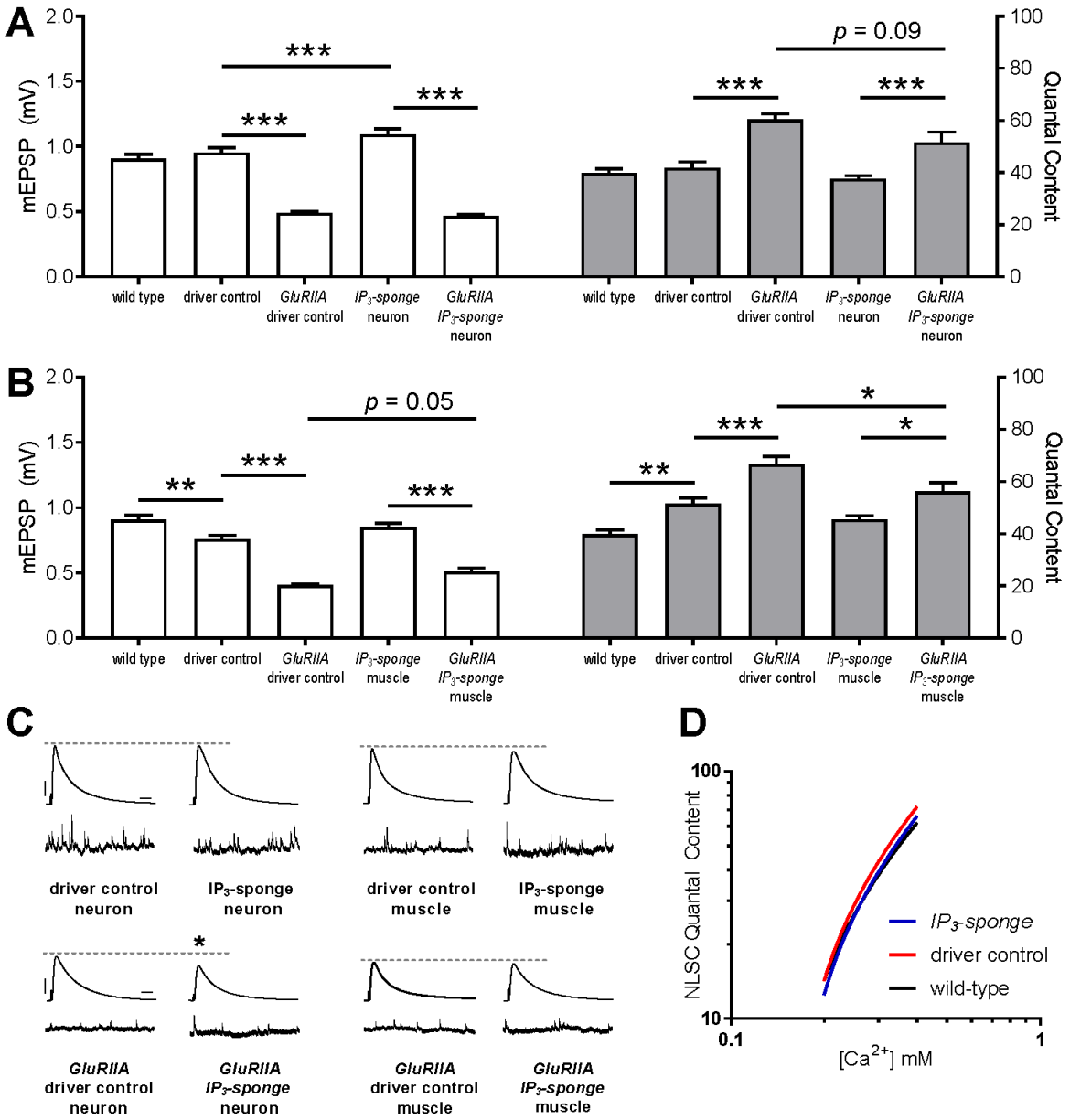

Figure 6: Combined pre-and postsynaptic IP_3 signaling maintains PHP.
(A-B) *IP_3-sponge* expression in single tissues (neuron or muscle) impairs PHP maintenance, but does not block it. For (A), NMJ electrophysiology data for neuronal *IP_3-sponge* expression driven by *elaV(C155)-Gal4.* For (B), NMJ electrophysiology data for muscle *IP_3-sponge* expression driven by *BG57-Gal4.* **(C)** Representative electrophysiological traces (EPSPs above; mEPSPs below) for the conditions in (A) and (B). **(D)** The calcium cooperativity of release is unaffected at the NMJ in the context of dual-tissue *IP_3-sponge* expression (linear regression analysis). Data on bar graphs are mean ± SEM. * $p < 0.05$, ** $p < 0.01$, *** $p < 0.001$ by one-way ANOVA followed by Bonferroni post-hoc test across genotypes shown. Scale bars for all traces are y = 10 mV (1 mV), x = 20 ms (500 ms) for EPSPs (mEPSPs).

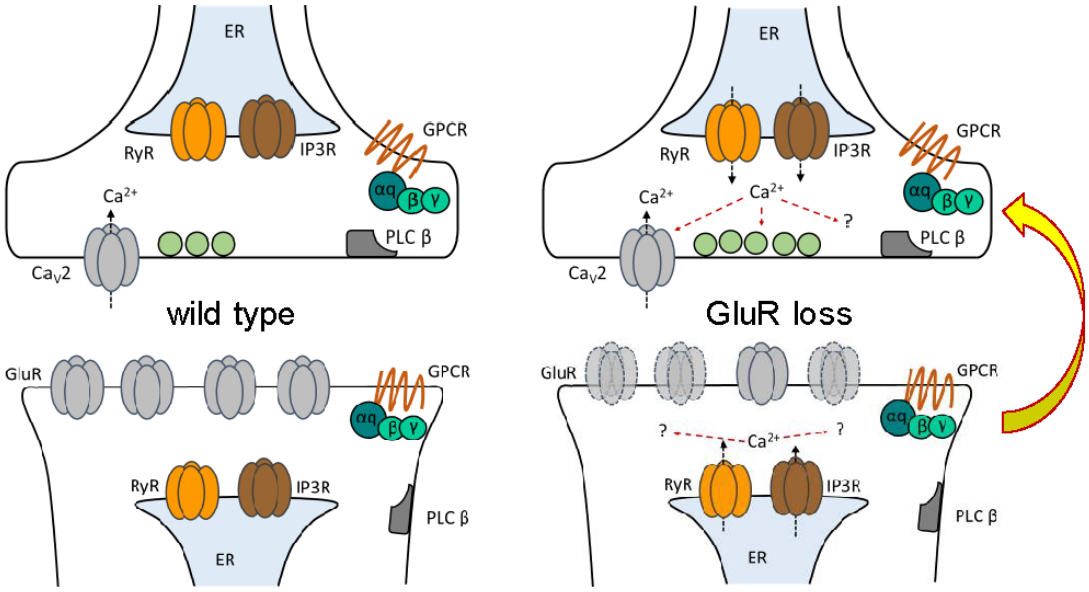

Figure 7. Model depicting PLCβ/IP3R/RyR signaling underling the maintenance of PHP in both muscle and neuron.

At the Drosophila NMJ, PLCβ and downstream effectors IP_3R and RyR are required for the maintenance of HSP. Left: PLCβ signaling components depicted in both muscle and neuron at the Drosophila NMJ. We detected no apparent role for PLCβ, IP3R, or RyR in baseline neurotransmission. Right: Reduced postsynaptic glutamate receptor function, either due to deletion of the *GluRIIA* gene or expression of *UAS-GluRIII[RNAi]*, initiates PHP. A retrograde, muscle-to-nerve signal instructs the neuron to increase the number of neurotransmitter vesicles released (quantal content). Our data support a model in which long-term maintenance of PHP requires PLCβ and its effectors in both the presynaptic neuron and postsynaptic muscle

Supplementary Tables S1-S5. Raw Electrophysiological Data. Genotypes and rearing conditions for electrophysiological data presented in the study (corresponding figures specified). For GAL4 drivers, "*Pre + Post-Gal4*" denotes a genetic combination of *elaV(C155)-Gal4/Y; Sca-Gal4/+; BG57-Gal4/+* (see Materials and Methods). Average values ± SEM are presented for each electrophysiological parameter, with *n* = number of NMJs recorded. Values include miniature excitatory postsynaptic potential (mEPSP) amplitude, mEPSP frequency (Freq), excitatory postsynaptic potential (EPSP) amplitude, quantal content (QC), and QC corrected for non-linear summation (NLS). * $p < 0.05$, ** $p < 0.01$, *** $p < 0.001$ by Student's t-test vs. unchallenged control.

Supplementary Table S1

FIGURE 1								
Gene	**Reagent**	**mEPSP (mV)**	**mEPSP freq. (Hz)**	**EPSP (mV)**	**V_m (mV)**	**QC**	**NLSC QC**	**n**
Driver control	*Pre + Post-Gal4*	0.83 ± 0.03	1.0 ± 0.1	40.4 ± 1.4	-69.0 ± 1.2	48.6 ± 1.1	100.2 ± 3.7	13
PhTox + Driver control	*Pre + Post-Gal4* >> + PhTox	0.59 ± 0.04	0.5 ± .01	40.5 ± 1.0	-67.0 ± 0.9	70.5 ± 4.3 ***	150.6 ± 10.7 ***	11
GluRIII	*Pre + Post-Gal4* >> *UAS-GluRIII RNAi/+*	0.64 ± 0.03	0.4 ± 0.0	37.5 ± 1.2	-70.1 ± 1.2	58.9 ± 2.1 *** (vs. Driver control)	110.6 ± 5.7	13
GluRIII	*Pre + Post-Gal4* >> *UAS-GluRIII RNAi/+* + PhTox	0.37 ± 0.01	0.2 ± 0.0	29.6 ± 1.0	-65.8 ± 0.8	80.1 ± 3.5 *** (vs. *GluRIII* alone)	133.2 ± 7.6	15
wild type		0.78 ± 0.02	2.0 ± 0.1	36.6 ± 0.7	-67.1 ± 0.6	48.3 ± 1.3	93.3 ± 3.0	57
wild type	+ PhTox	0.53 ± 0.02	0.8 ± 0.1	33.3 ± 0.7	-64.4 ± 0.3	65.1 ± 2.8 ***	119.7 ± 6.3 ***	24
PLC21C (*GluRIII* cont)	*Pre + Post-Gal4* >> *GD11359*	0.80 ± 0.04	1.3 ± 0.1	34.9 ± 1.4	-67.4 ± 1.4	44.7 ± 2.8	83.7 ± 6.9	14
PLC21C	*Pre + Post-Gal4* >> *GD11359/+ GluRIII RNAi/+*	0.55 ± 0.01	0.3 ± 0.0	29.6 ± 1.0	-66.0 ± 0.7	53.9 ± 0.5 * (vs. *Plc21C RNAi*)	89.4 ± 5.0	17
PLC21C	*Pre + Post-Gal4* >> *GD11359/+ GluRIII RNAi/+* + PhTox	0.42 ± 0.01	0.2 ± 0.1	27.3 ± 1.7	-64.9 ± 1.2	64.9 ± 4.1 * (vs. *Plc21C* + *GluRIII RNAi*)	105.1 ± 10.4	11
PLC21C (PhTox cont)	*Pre + Post-Gal4* >> *GD11359*	0.80 ± 0.04	0.7 ± 0.1	31.6 ± 0.9	-66.0 ± 0.9	40.6 2.0 ***	69.8 ± 6.5	14
PLC21C	*Pre + Post-Gal4* >> *GD11359/+* + PhTox	0.51 ± 0.01	0.3 ± 0.1	30.9 ± 1.7	-66.5 ± 0.9	61.1 ± 3.7 ***	106.8 ± 9.5 **	14

Supplementary Table S2

FIGURE 2 – SCREEN								
Gene	**Reagent**	**mEPSP (mV)**	**mEPSP freq. (Hz)**	**EPSP (mV)**	**V_m (mV)**	**QC**	**NLSC QC**	**n**
wild type	*w^{1118}*	0.88 ± 0.02	3.3 ± 0.2	38.3 ± 0.7	-68.2 ± 0.7	44.1 ± 1.0	87.6 ± 2.7	52
GluRIIA	*$GluRIIA^{SP16}$*	0.46 ± 0.02	0.9 ± 0.1	29.2 ± 1.0	-68.7 ± 0.8	66.0 ± 3.1 ***	107.3 ± 6.2 ***	24
GluRIII RNAi	*Pre + Post-Gal4*	0.81 ± 0.02	2.0 ± 0.7	37.5 ± 1.3	-68.3 ± 1.0	46.7 ± 1.7	91.9 ± 5.0	22
	Pre + Post-Gal4 >> GluRIII RNAi/+	0.57 ± 0.02	0.3 ± 0.0	34.1 ± 0.8	-67.6 ± 1.0	60.5 ± 1.9 ***	108.3 ± 3.9 *	17
CG7611	*$CG7611^{EY07631}$*	0.93 ± 0.03	3.3 ± 0.3	28.3 ± 1.3	-67.3 ± 0.9	30.9 ± 1.7	49.6 ± 3.4	12
	$GluRIIA^{SP16}$; $CG7611^{EY07631}$	0.45 ± 0.02	1.6 ± 0.2	23.6 ± 1.7	-67.1 ± 1.0	53.1 ± 4.4 ***	79.6 ± 8.8 **	13
Mipp2	*Pre + Post-Gal4 >> TRiP.HMC03229*	0.98 ± 0.04	1.1 ± 0.2	36.4 ± 1.5	-69.8 ± 1.6	37.4 ± 1.5	69.5 ± 3.9	10
	Pre + Post-Gal4 >> TRiP.HMC03229 + GluRIII RNAi	0.65 ± 0.03	0.2 ± 0.0	33.7 ± 1.2	-68.1 ± 1.2	52.5 ± 2.3 ***	92.6 ± 4.7 **	9
Mipp2	*Pre + Post-Gal4 >> 4317-R2*	0.82 ± 0.03	0.8 ± 0.1	43.9 ± 1.7	-71.4 ± 1.4	53.9 ± 2.3	118.9 ± 8.6	11
	Pre + Post-Gal4 >> 4317-R2 + GluRIII RNAi	0.60 ± 0.03	0.4 ± 0.0	37.0 ± 1.6	-71.7 ± 1.1	62.0 ± 2.0 *	113.9 ± 5.1	10
Mipp2	*$Mipp2^{KG01786}$*	0.97 ± 0.04	1.7 ± 0.2	39.0 ± 1.1	-69.8 ± 1.1	40.8 ± 1.7	81.1 ± 4.5	15
	$Mipp2^{KG01786}$; $GluRIIA^{SP16}$	0.52 ± 0.03	1.1 ± 0.2	29.6 ± 1.7	-71.7 ± 1.1	57.2 ± 3.4 ***	92.4 ± 6.9	16
slowpoke	*slo^4*	0.83 ± 0.08	5.0 ± 0.1	36.3 ± 1.6	-71.3 ± 1.0	47.7 ± 2.8	87.0 ±5.6	18
	$GluRIIA^{SP16}$; slo^4	0.42 ± 0.02	1.7 ± 0.1	26.0 ± 1.7	-70.3 ± 1.0	64.1 ± 5.2 *	100.4 ± 9.4	22
slowpoke	*slo^4/slo^1*	0.93 ± 0.05	3.7 ± 0.4	35.9 ± 1.2	-69.9 ± 0.9	40.1 ± 2.2	73.9 ± 4.5	19
	$GluRIIA^{SP16}$; slo^4/slo^1	0.38 ± 0.01	1.4 ± 0.2	25.4 ± 1.6	-70.8 ± 0.9	67.5 ± 4.0 ***	102.6 ± 8.7 ***	18
Gβ13F	*$Gβ13F^{KG08410}$*	0.97 ± 0.06	1.4 ± 0.2	26.9 ± 1.9	-63.2 ± 0.4	28.1 ± 2.3	45.6 ± 4.9	8
	$GluRIIA^{SP16}$; $Gβ13F^{KG08410}$	0.52 ± 0.01	2.6 ± 0.6	31.8 ± 1.5	-66.2 ± 0.1	61.1 ± 2.6 ***	106.0 ± 7.2 ***	7
Gβ76C	*$Gβ76C^1$*	0.99 ± 0.05	1.0 ± 0.1	39.6 ± 0.9	-69.8 ± 1.1	40.6 ± 1.9	80.9 ± 4.0	7
	$GluRIIA^{SP16}$; $Gβ76C^1$	0.50 ± 0.02	0.7 ± 0.1	29.6 ± 2.0	-71.9 ± 2.6	59.4 ± 2.6 ***	93.9 ± 6.5	8
Gβ76C	*Pre + Post-Gal4 >> GD 13785*	0.73 ± 0.04	0.4 ± 0.0	41.1 ± 1.4	-70.3 ± 0.9	57.9 ± 3.3	120.1 ± 7.8	13

	Pre + Post-Gal4 >> GD 13785 GluRIII RNAi	0.54 ± 0.02	0.3 ± 0.0	34.5 ± 1.4	-69.3 ± 1.7	64.7 ± 0.7	115.6 ± 2.6	16
TkR86C	*Pre + Post-Gal4 >> TRiP.JF02160*	1.00 ± 0.06	0.4 ± 0.1	36.7 ± 2.0	-66.7 ± 0.8	38.5 ± 3.6	77.5 ± 9.8	10
	Pre + Post-Gal4 >> GluRIII RNAi/ *TRiP.JF02160*	0.78 ± 0.02	0.3 ± 0.0	41.2 ± 1.1	-66.9 ± 1.5	52.6 ± 2.0 **	113.9 ± 5.7 **	8
mAChR-A	*Pre + Post-Gal4 >> TRiP.HMC02343*	0.97 ± 0.03	1.1 ± 0.2	37.1 ± 1.1	-66.3 ± 0.6	38.7 ± 1.5	76.2 ± 4.2	14
	Pre + Post-Gal4 >> TRiP.HMC02343 + GluRIII RNAi	0.71 ± 0.03	0.1 ± 0.0	34.1 ± 1.5	-66.7 ± 0.8	48.5 ± 1.5 ***	88.3 ± 4.3 *	13
GABA-B-R1	*Pre + Post-Gal4 >> TRiP.HMC03388*	1.00 ± 0.05	0.7 ± 0.1	39.6 ± 1.4	-69.8 ± 0.7	40.1 ± 1.5	80.2 ± 3.9	7
	Pre + Post-Gal4 >> TRiP.HMC03388 + GluRIII RNAi	0.78 ± 0.02	0.3 ± 0.0	35.1 ± 0.8	-66.5 ± 1.2	45.1 ± 1.4 *	83.5 ± 3.1	8
PK2-R2	*Pre + Post-Gal4 >> TRiP.JF03209*	1.02 ± 0.05	1.6 ± 0.5	36.0 ± 1.6	-67.1 ± 1.0	35.7 ± 0.9	67.3 ± 2.4	8
	Pre + Post-Gal4 >> TRiP.JF03209 + GluRIII RNAi	0.80 ± 0.04	0.8 ± 0.1	35.2 ± 1.8	-64.5 ± 0.8	44.2 ± 1.9 **	85.1 ± 5.6 *	9
methuselah	*Pre + Post-Gal4 >> TRiP.GL01060*	0.81 ± 0.03	1.1 ± 0.2	37.5 ± 1.5	-68.2 ± 1.1	46.9 ± 2.0	91.7 ± 5.5	15
	Pre + Post-Gal4 >> TRiP.GL01060 + GluRIII RNAi	0.66 ± 0.03	0.4 ± 0.1	36.7 ± 1.3	-70.5 ± 1.1	56.4 ± 1.9 **	105.3 ± 5.2	13
AdoR	*Pre + Post-Gal4 >> TRiP.JF02687*	0.89 ± 0.05	1.5 ± 0.2	33.1 ± 1.7	-69.3 ± 1.3	37.8 ± 2.5	65.8 ± 5.7	8
	Pre + Post-Gal4 >> TRiP.JF02687 + GluRIII RNAi	0.69 ± 0.03	0.6 ± 0.1	32.5 ± 1.9	-67.6 ± 1.8	46.9 ± 2.4 *	81.7 ± 5.9	9
PKC	*Pre + Post-Gal4 >> UAS-PKCi.B*	0.79 ± 0.04	1.0 ± 0.2	35.7 ± 1.7	-70.3 ± 1.5	45.9 ± 2.1	83.6 ± 5.2	14
	Pre + Post-Gal4 >> UAS-PKCi.B + GluRIII RNAi	0.62 ± 0.03	0.2 ± 0.0	33.5 ± 1.0	-66.7 ± 1.2	55.4 ± 3.1 *	100.8 ± 8.0	14
unc-13	*Pre + Post-Gal4 >> KK109346*	1.12 ± 0.04	2.6 ± 0.2	41.6 ± 1.7	-73.0 ± 1.4	37.5 ± 1.6	77.0 ± 4.7	15
	Pre + Post-Gal4 >> KK109346 + GluRIII RNAi	0.88 ± 0.03	0.8 ± 0.1	39.8 ± 1.2	-68.6 ± 0.8	45.4 ± 1.1 ***	92.7 ± 3.6 *	15
iav	*Pre + Post-Gal4 >> TRiP.JF01904*	0.89 ± 0.03	0.9 ± 0.1	35.9 ± 1.0	-70.7 ± 1.2	40.6 ± 1.4	73.8 ± 3.3	14
	Pre + Post-Gal4 >> TRiP.JF01904 + GluRIII RNAi	0.70 ± 0.16	0.4 ± 0.1	32.1 ± 1.2	-67.7 ± 1.0	45.6 ± 1.6 *	78.7 ± 4.1	14
Slip1	*Pre + Post-Gal4 >> TRiP.HMC03268*	0.70 ± 0.03	0.9 ± 0.1	31.2 ± 1.6	-65.7 ± 0.6	45.2 ± 3.2	79.2 ± 8.0	11

	Pre + Post-Gal4 >> TRiP.HMC03268 + GluRIII RNAi	0.56 ± 0.03	0.3 ± 0.0	33.1 ± 1.9	-67.7 ± 1.0	59.6 ± 3.1 **	105.7 ± 8.3 *	9
mGluR	*mGluR*^{MI02169}	1.01 ± 0.05	7.0 ± 0.8	36.0 ± 1.1	-64.3 ± 0.7	36.0 ± 2.3	70.5 ± 5.9	6
	GluRIIA^{SP16}*;;mGluR*^{MI02169}	0.45 ± 0.01	1.7 ± 0.9	28.7 ± 1.6	-63.0 ± 0.7	64.4 ± 4.3 ***	108.8 ± 11.7	7
Pka-R2	*Pre + Post-Gal4 >> TRiP.JF02759*	0.79 ± 0.04	1.0 ± 0.1	35.0 ± 1.4	-64.9 ± 0.5	44.7 ± 1.7	84.5 ± 4.4	8
	Pre + Post-Gal4 >> TRiP.JF02759	0.58 ± 0.03	2.7 ± 2.4	31.4 ± 1.9	-64.8 ± 1.5	54.3 ± 2.6 **	94.6 ± 6.9	7
Gβ5	*Pre + Post-Gal4 >> TRiP.JF02941*	1.15 ± 0.07	1.6 ± 0.2	39.4 ± 1.7	-70.6 ± 2.2	35.0 ± 1.8	69.0 ± 4.0	13
	Pre + Post-Gal4 >> TRiP.JF02941 GluRIII RNAi	0.80 ± 0.06	0.3 ± 0.1	39.9 ± 1.8	-69.5 ± 1.1	50.6 ± 1.9 ***	102.0 ± 4.3 ***	11
CaMKII (presynaptic)	*Pre-Gal4 >> UAS-CaMKII-Ala*	0.90 ± 0.03	2.0 ± 0.2	38.3 ± 1.5	-69.3 ± 1.0	43.2 ± 1.9	85.0 ± 5.4	15
	Pre-Gal4 >> UAS-CaMKII-Ala, GluR/GluR	0.51 ± 0.02	0.8 ± 0.1	28.3 ± 1.7	-67.4 ± 1.1	56.6 ± 3.5 **	91.1 ± 7.2	11
	Pre-Gal4 >> UAS-CaMKII-Ala + PhTox	0.53 ± 0.02	1.2 ± 0.1	31.9 ± 2.6	-66.5 ± 1.0	62.1 ± 6.3 ***	113.66 ± 16.33	9
UAS-IP$_3$-sponge.m49	*Pre + Post-Gal4 >> UAS-IP3-sponge.m49*	0.89 ± 0.04	1.3 ± .01	43.1 ± 1.7	-69.3 ± 1.3	49.1 ± 2.0	111.1 ± 8.7	13
	Pre + Post-Gal4 >> UAS-IP$_3$-sponge.m49 + GluRIII RNAi	0.55 ± 0.03	0.3 ± 0.1	28.5 ± 1.4	-64.4 ± 0.5	52.4 ± 2.4	86.4 ± 5.2 *	14
UAS-IP$_3$-sponge.m30	*Pre + Post-Gal4 >> UAS-IP$_3$-sponge.m30*	0.81 ± 0.04	1.4 ± 0.2	43.8 ± 1.4	-69.4 ± 1.6	55.1 ± 1.8	123.3 ± 4.6	16
	Pre + Post-Gal4 >> UAS-IP$_3$-sponge.m30 + GluRIII RNAi	0.63 ± 0.02	0.3 ± 0.0	34.6 ± 1.1	-67.2 ± 0.9	55.5 ± 2.3	102.0 ± 5.4 ** (down)	15
UAS-IP$_3$-sponge.m49 (PhTox)	*Pre + Post-Gal4 >> UAS-IP$_3$-sponge.m49* (PhTox Cont)	0.90 ± 0.03	1.6 ± 0.2	40.1 ± 1.3	-67.4 ± 1.0	45.2 ± 2.4	96.5 ± 7.8	13
	Pre + Post-Gal4 >> UAS-IP$_3$-sponge.m49 PhTox	0.54 ± 0.02	1.0 ± 0.1	38.6 ± 2.4	-65.3 ± 0.9	73.1 ± 5.0 ***	163.2 ± 17.6 **	15
UAS-IP$_3$-sponge.m49	*Pre + Post-Gal4 >> UAS-IP$_3$-sponge.m49 + GluRIII* RNAi	0.66 ± 0.03	0.4 ± 0.1	31.7 ± 1.2	-64.9 ± 0.7	48.9 ± 1.8	86.4 ± 4.7	16
	Pre + Post-Gal4 >> UAS-IP$_3$-sponge.m49 + GluRIII RNAi PhTox	0.40 ± 0.02	0.2 ± 0.0	27.5 ± 1.8	-64 ± 0.7	69.9 ± 4.9 ***	116.1 ± 12.1 *	14

Supplementary Table S3

FIGURE 4								
Gene	**Reagent**	**mEPSP (mV)**	**mEPSP freq. (Hz)**	**EPSP (mV)**	**V_m (mV)**	**QC**	**NLSC QC**	**n**
wild type	5 μM Xestospongin C	0.85 ± 0.04	3.1 ± 0.3	38.8 ± 1.1	-66.4 ± 0.9	46.3 ± 2.3	95.2 ±0.5	13
GluRIIA^{SP16}	5 μM Xestospongin C	0.46 ± 0.03	0.8 ± 0.1	28.5 ± 1.9	-68.2 ± 1.5	64.0 ± 4.3 *	104.3 ± 9.8	15
wild type	20 μM Xestospongin C	1.00 ± 0.04	6.1 ± 0.4	37.3 ± 0.8	-64.1 ± 0.6	37.7 ± 0.9	76.4 ± 2.5	14
wild type	20 μM PhTox + 20 μM Xestospongin C	0.56 ± 0.01	1.5 ± 0.2	34.2 ± 1.0	-64.6 ± 0.8	61.8 ± 1.6 ***	115.9 ± 4.9 ***	19
GluRIIA^{SP16}	20 μM Xestospongin C	0.54 ± 0.02	1.3 ± 0.2	21.4 ± 0.9	-64.1 ± 0.1	40.4 ± 2.1	57.4 ± 3.5 *** (down)	13
wild type (GluR cont)	1 μM 2-APB	0.80 ± 0.02	3.6 ± 0.3	35.9 ± 1.3	-68.0 ± 1.1	45.0 ± 1.3	85.2 ± 4.3	15
GluRIIA^{SP16}	1 μM 2-APB	0.53 ± 0.02	0.9 ± 0.1	23.4 ± 1.1	-67.2 ± 0.8	45.3 ± 2.6	66.4 ± 5.1 ** (down)	14
wild type (PhTox cont)	1 μM 2-APB	0.75 ± 0.02	2.9 ± 0.2	39.9 ± 1.2	-66.0 ± 0.9	53.5 ± 1.8	114.2 ± 6.0	11
wild type	1 μM 2-APB 20 μM PhTox	0.48 ± 0.04	1.6 ± 0.3	35.6 ± 1.8	-63.2 ± 0.5	76.9 ± 4.0 ***	152.3 ± 9.5 **	12
wild type	10 μM 2-APB	0.83 ± 0.03	4.7 ± 0.9	43.3 ± 0.8	-65.0 ± 0.7	53.3 ± 2.5	128.3 ± 8.1	15
GluRIIA^{SP16}	10 μM 2-APB	0.44 ± 0.02	0.7 ± 0.1	23.9 ± 1.0	-64.9 ± 0.6	54.9 ± 2.9	82.2 ± 5.8 ***	14
wild type	DMSO (2% v/v)	0.85 ± 0.04	5.4 ± 0.5	35.8 ± 1.2	-64.9 ± 0.8	42.8 ± 1.8	83.1 ± 4.5	12
GluRIIA^{SP16}	DMSO (2% v/v)	0.46 ± 0.02	1.21 ± 0.16	26.1 ± 1.1	-65.2 ± 0.7	57.5 ± 3.4 ***	89.5 ± 7.0	11
wild type	PhTox + DMSO (2% v/v)	0.56 ± 0.02	1.9 ± 0.2	35.7 ± 1.0	-67.0 ± 1.1	64.5 ± 2.6 ***	121.2 ± 5.7 ***	15

Supplementary Table S4

FIGURE 5								
Gene	**Reagent**	**mEPSP (mV)**	**mEPSP freq. (Hz)**	**EPSP (mV)**	**V_m (mV)**	**QC**	**NLSC QC**	**n**
wild type	+100 μM Ryanodine	0.78 ± 0.02	3.7 ± 0.3	34.6 ± 1.1	-66.4 ± 0.9	45.0 ± 2.2	84.1 ± 5.4	17
GluRIIA^{SP16}	+100 μM Ryanodine	0.50 ± 0.01	1.3 ± 0.1	25.4 ± 1.1	-66.2 ± 0.8	51.5 ± 2.4	78.4 ± 4.8	15
wild type	+10 μM dantrolene	0.81 ± 0.04	3.2 ± 0.2	29.2 ± 1.6	-64.3 ± 0.5	37.3 ± 2.4	65.0 ± 5.1	25
GluRIIA^{SP16}	+10 μM dantrolene	0.46 ± 0.01	0.9 ± 0.1	15.9 ± 1.3	-64.8 ± 0.6	34.7 ± 2.9	46.5 ± 4.7 **	27
wild type	+10 μM dantrolene	0.91 ± 0.04	2.6 ± 0.2	34.8 ± 1.6	-64.2 ± 0.7	39.4 ± 2.6	76.5 ± 6.5	13
wild type	+PhTox +10 μM dantrolene	0.53 ± 0.02	1.4 ± 0.2	34.4 ± 1.3	-64.7 ± 0.9	66.1 ± 4.8 ***	126.3 ± 13.7 **	10
GluRIII RNAi	*Pre + Post-Gal4 >>* GluRIII RNAi +20 μM PhTox +10 μM dantrolene	0.39 ± 0.03	0.4 ± 0.1	36.2 ± 1.5	-67.4 ± 1.2	96.5 ± 6.0 **	183.8 ± 13.7 *	11
Driver Control	*Pre + Post-Gal4 >>* +10 μM Dantrolene	0.73 ± 0.03	0.9 ± 0.1	39.9 ± 1.8	-67.6 ± 0.9	55.5 ± 2.7	118.2 ± 9.5	14
GluRIII RNAi	*Pre + Post-Gal4 >>* *GluRIII* RNAi/+ 10 μM Dantrolene	0.61 ± 0.02	0.2 ± 0.0	31.5 ± 1.0	-65.5 ± 0.9	52.6 ± 2.2	90.8 ± 4.7	14
GluRIII RNAi *IP_3 sponge*	*Pre + Post-Gal4 >>* *GluRIII* RNAi/*UAS-IP_3-sponge.m49* 10 μM Dantrolene	0.68 ± 0.05	0.4 ± 0.1	33.3 ± 1.8	-66.0 ± 1.1	50.3 ± 2.1	90.5 ± 4.3	13
Driver Control *IP_3 sponge*	*Pre + Post-Gal4 >>* *UAS-IP_3-sponge.m49* 10 μM Dantrolene	0.93 ± 0.03	1.6 ± 0.1	41.2 ± 1.7	-67.6 ± 1.4	44.5 ± 1.5	96.1 ± 5.8	12

Supplementary Table S5

FIGURE 6								
Gene	**Reagent**	**mEPSP (mV)**	**mEPSP freq. (Hz)**	**EPSP (mV)**	**V_m (mV)**	**QC**	**NLSC QC**	**n**
Driver Control (Neuron)	*Pre-Gal4*	0.95 ± 0.04	2.6 ± 0.2	38.7 ± 1.1	-66.5 ± 1.0	41.9 ± 2.3	86.2 ± 5.8	17
	Pre-Gal4 *GluRIIA^{SP16}*	0.49 ± 0.01	1.3 ± 0.2	29.5 ± 1.2	-65.1 ± 0.7	60.3 ± 2.2 ***	101.2 ± 6.1	15
IP$_3$-sponge	*Pre-Gal4 >>* *UAS-IP$_3$-sponge.m49*	1.09 ± 0.04	3.5 ± 0.0	40.8 ± 1.5	-69.9 ± 1.3	37.6 ± 1.3	77.9 ± 3.7	16
GluRIIA *IP$_3$-sponge*	*Pre-Gal4 >>* *UAS-IP$_3$-sponge.m49* *GluRIIA^{SP16}*	0.47 ± 0.01	0.6 ± 0.1	24.3 ± 2.1	-68.4 ± 1.1	51.6 ± 4.0 **	79.2 ± 9.4	15
Driver Control (Muscle)	Post-Gal4	0.76 ± 0.0	2.8 ± 0.2	38.7 ± 1.0	-67.6 ± 1.0	51.6 ± 2.1	103.6 ± 5.3	14
	Post-Gal4 *GluRIIA^{SP16}*	0.41 ± 0.01	0.7 ± 0.1	26.8 ± 1.0	-66.2 ± 0.8	66.7 ± 3.0 ***	105.4 ± 6.6	14
IP$_3$-sponge	*Post-Gal4 >>* *UAS-IP$_3$-sponge.m49*	0.85 ± 0.03	2.1 ± 0.2	38.3 ± 1.1	-65.7 ± 0.7	45.4 ± 1.5	93.6 ± 4.8	15
GluRIIA *IP$_3$-sponge*	*Post-Gal4 >>* *UAS-IP$_3$-sponge.m49* *GluRIIA^{SP16}*	0.51 ± 0.03	1.4 ± 0.2	27.8 ± 1.3	-65.3 ± 0.9	56.2 ± 0.7 **	92.1 ± 7.9	16